4-1970

Elastic Scattering of 1.33 MeV Gamma Rays from Uranium

Joan Sue De Vries
Western Michigan University

ELASTIC SCATTERING OF 1.33 MeV GAMMA RAYS FROM URANIUM

by

Joan Sue De Vries

A Thesis
Submitted to the
Faculty of the School of Graduate
Studies in partial fulfillment
of the
Degree of Master of Arts

Western Michigan University
Kalamazoo, Michigan
April, 1970

ACKNOWLEDGEMENTS

Gratitude and appreciation are expressed to Professor Gerald Hardie for his guidance in performing the experiment and theoretical calculations discussed in this thesis. Thanks are also due to the staff of the Western Michigan University Computer Center for their advice and cooperation.

Thanks is also expressed to Mr. H. Heystek of Kalamazoo Radiology for developing our x-ray films.

The help of my co-worker, Chwan-kang Chiang, was also greatly appreciated.

Joan Sue De Vries

MASTER'S THESIS M-2282

DE VRIES, Joan Sue
ELASTIC SCATTERING OF 1.33 MeV GAMMA RAYS FROM URANIUM.

Western Michigan University, M.A., 1970
Physics, nuclear

University Microfilms, A XEROX Company, Ann Arbor, Michigan

TABLE OF CONTENTS

TABLES AND FIGURES

INTRODUCTION

In the early part of the twentieth century, it was thought that the elastic scattering of gamma rays from an atom arose from Thomson scattering from the nucleus and Rayleigh scattering from the electrons. With the development of quantum electrodynamics it was postulated that an additional process, called Delbruck scattering, would occur. However, this has yet to be verified experimentally.

Delbruck theory predicts that, upon entry into the strong Coulomb field surrounding the nucleus, a photon may create either a real or a virtual electron-positron pair. The pair annihilates creating a photon which leaves at an angle θ with respect to the initial photon's direction. The real pair corresponds to the imaginary part of the Delbruck amplitude and the virtual pair is associated with the real part of the Delbruck amplitude; the latter pair is of special interest. Such an effect, if present, should make a small contribution to the elastic scattering cross section.

Establishment of the presence of this small effect requires that the experimental error be less than the magnitude of the effect and that accurate calculations of the contributions of the other processes to the elastic scattering cross section can be made.

This thesis presents a more accurate cross section measurement done with a lithium-drifted germanium crystal for higher energy resolution than was possible in previous experiments. The accurate calculation of the contributions of the other scattering processes continues to be a major problem. Two problems must be solved: how can the Rayleigh amplitudes, which have been calculated for an energy of 1.31 MeV and a mercury scatterer, be extrapolated to the present case and which amplitudes should be included in the cross section. Cross sections composed of different amplitudes and extrapolations were calculated and compared to the experimental data to determine which amplitudes should be included in the best theoretical curve.

THEORY

When gamma rays react with matter they can be either absorbed, scattered elastically or scattered inelastically.

The absorption consists of two processes. The first, the photoelectric effect, occurs when the incoming photon strikes a bound electron in the target atom. The electron leaves the atom with the energy of the incoming photon less the binding energy of the electron. This effect is predominant at lower energies. In the second process, pair production, the photon annihilates into a positron and an electron in the field of the nucleus. Although this effect increases with increasing photon energy , it is much less probable than the Compton effect at 1.33 MeV.

The inelastic scattering consists mainly of Compton scattering, which is scattering from a loosely bound or a free electron. The photon collides with an electron losing some of its energy. The Compton scattering cross section can be calculated by the Klein-Nishina formula[1]. Conservation of energy and momentum permit one to calculate the energy of the scattered photon; the energy approaches the incident photon's energy as the scattering angle approaches zero.

The elastic scattering consists of four processes: nuclear Thomson, Rayleigh, Delbruck, and nuclear resonance scattering. To obtain the elastic scattering cross section, the amplitudes of these processes must be added coherently.

Thomson scattering is Compton scattering of the photons from the nucleus; since the mass of the nucleus is so large, the photon scatters with negligible energy loss. Rayleigh scattering is elastic scattering from tightly bound electrons; the electrons remain bound and in the same shell. The Rayleigh amplitudes are usually calculated only for the electrons in the K-shell although it has been shown[2] that the L-shell also makes a contribution to the cross section. Delbruck scattering, sometimes called "nuclear potential scattering", is due to electron-positron pair creation and annihilation. The amplitudes of these three processes are discussed in Appendix B for lead and uranium scatterers.

There remains a fourth type of scattering, nuclear resonance scattering, in which the incident photon excites a nuclear level, with the subsequent reemission of the excitation energy. This was investigated both by Levinger[3] and Chiang[4] and found to be negligible for lead and uranium scatterers.

APPARATUS AND PROCEDURE

The apparatus consisted primarily of three parts: the source of gamma rays, the uranium target, and the system detecting the scattered gamma rays. These are shown in Figure I.

The beam of gamma rays was provided by an 111 Curie ^{60}Co source housed in 1.5 tons of lead. The beam was controlled by a mercury shutter. The mercury, which normally blocked the beam, could be forced up into a reservoir by compressed nitrogen gas, thereby exposing the source. To block the beam the gas was released, causing the mercury to return to its original position.

The target consisted of a slab of uranium of dimensions 16.5 cm by 14.5 cm which was hung a distance r from the source. The target was suspended from an aluminum bar which was located above and in front of the source. This bar could be pivoted over an aluminum disc which was marked in degrees and previously aligned with the photon beam using a laser. A final check on the position of the target in relationship to the beam was made by placing a piece of x-ray film behind the target and opening the source. The exposed film revealed the shadow of the target and the area of the beam.

The gamma ray detection system consisted of an 11 cm^3 active volume, lithium-drifted germanium crystal and a conventional arrangement of electronics. The electronic arrangement is shown in Figure II.

The differential scattering cross section at a scattering angle θ,

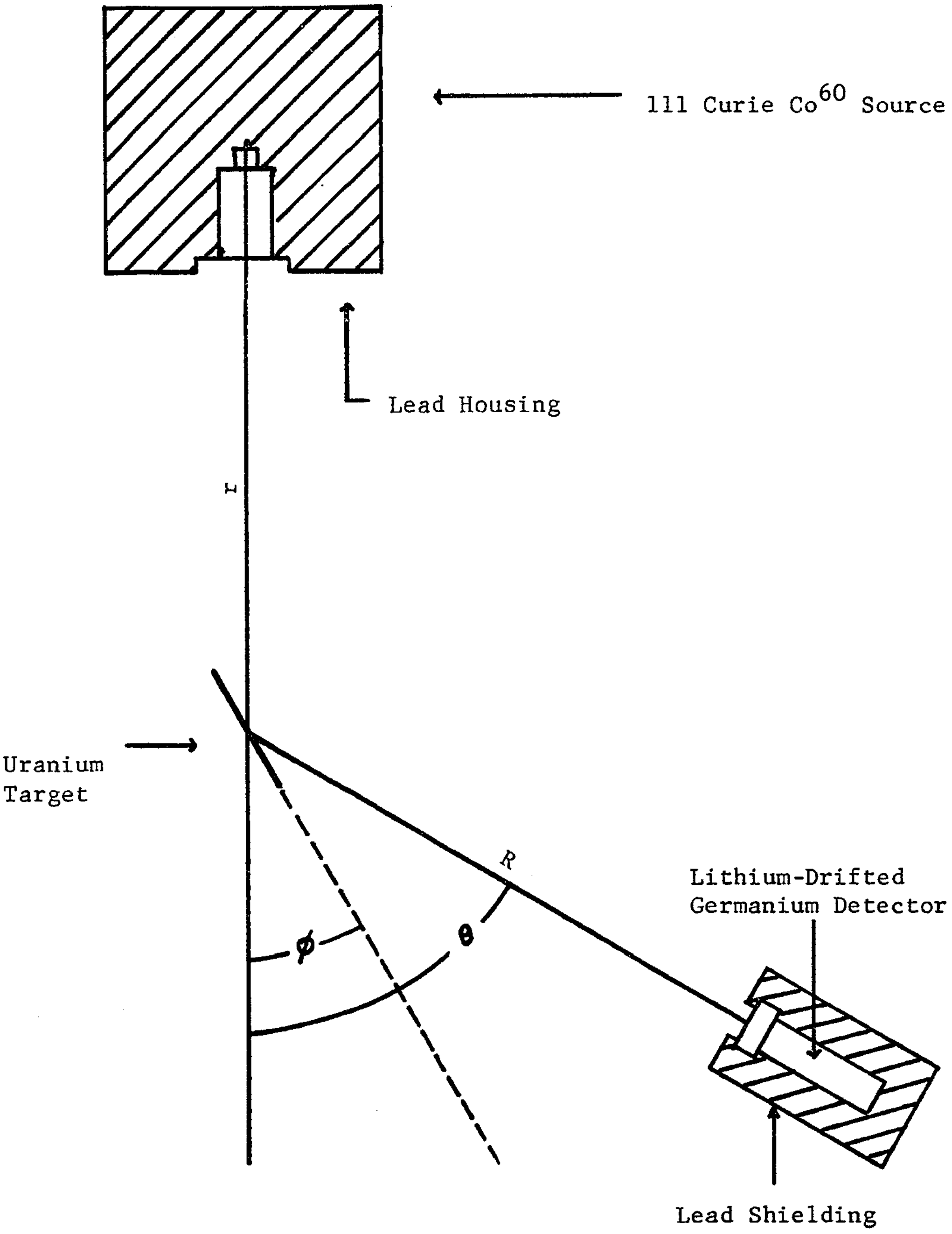

Figure I. Experimental arrangement for scattering angle $\theta = 60°$.

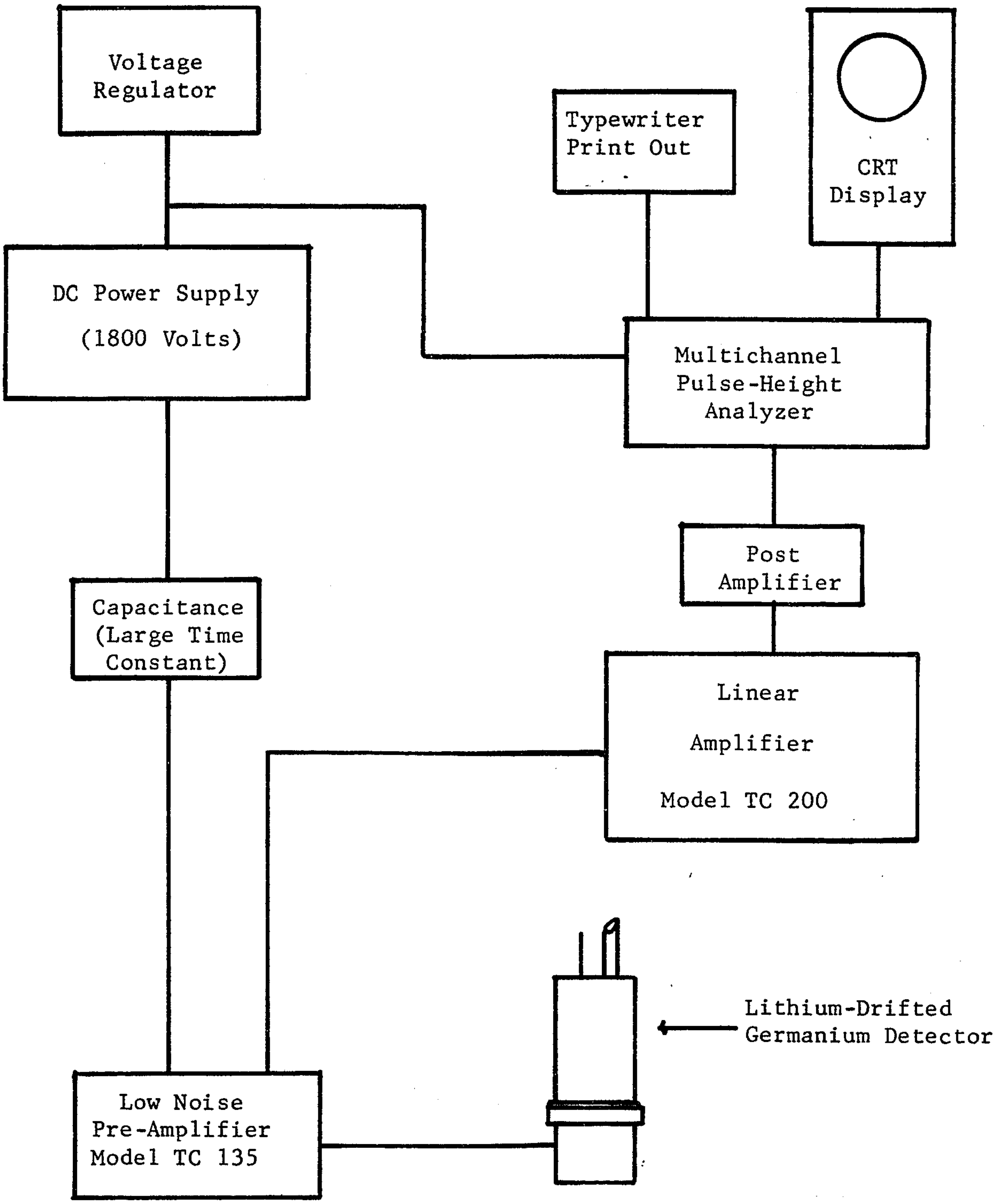

Figure II. Lithium-Germanium Spectrometer

$\left(\frac{d\sigma}{d\Omega}\right)_\theta$, was obtained by making two measurements. First the number of events per second, n_a, in the full energy peak was obtained. This is related to the cross section by[5]

$$n_a = \frac{a}{4\pi r^2} N_o \left(\frac{d\sigma}{d\Omega}\right)_\theta \omega \epsilon C$$

where a is the number of gamma rays emitted per second by the source at 1.33 MeV, r is the source to target distance, N_o is the number of target atoms, ω is the solid angle subtended by the counter at the target, ϵ is the probability of the gamma ray elastically scattered within the solid angle ω losing all its energy in the detector, and C is the correction for absorption of gamma rays in the target and variation of gamma ray flux over the surface of the target.

The measurement of ω and ϵ, which is difficult to perform accurately, was eliminated by making a second measurement using an auxiliary source. This auxiliary source consisted of a piece of cardboard, equal in size to the target, which had been painted uniformly with a liquid containing ^{60}Co. When this is hung in place of the target, the main source being closed, the counting rate, n_b, is given by

$$n_b = b \frac{\omega}{4\pi} \epsilon$$

where b is the auxiliary source strength.

The ω and ϵ in both equations are the same because the geometry is identical and because the gamma rays from both sources have the same energy. Therefore the two equations can be combined to give

$$\frac{d\sigma}{d\Omega} = \frac{n_a}{n_b} \frac{b}{a} \frac{r^2}{N_o} \frac{1}{C}$$

where b/a had to be determined in a separate experiment.[6]

At each angle for which the cross section was measured, the detector was aligned using the machined disc and the laser. To minimize the spread in scattering angle due to the finite size of the detector, the target was positioned at an angle ϕ which satisfied the relationship[7] $\frac{\sin\phi}{\sin(\theta-\phi)} = \frac{r}{R}$.

Shielding was positioned to minimize the detection of photons which were not scattered from the target. A sufficient thickness of lead was placed in front of the detector so that pile-up, caused by large numbers of Compton scattered gamma rays, was negligible.

At each angle the collection of data consisted first of a run with the auxiliary source in the target position, then two or three runs with the target in position and finally another run with the auxiliary source in position. Each run consisted of counting for a given live time, then subtracting background for the same live time. The total counting time for each target varied from 800 live minutes to 200 live minutes depending on the angle and the amount of lead absorber in front of the detector. This was sufficient to insure that counting statistics contributed an uncertainty of less than 3% in all cases.

CORRECTIONS

There are only two corrections which were significant in the calculation of the cross section. The first correction is for the variation in the source to scattering center distance over the surface of the target. This has been previously calculated to be[6]

$$\frac{1}{r^2} = \frac{1}{r_0^2}\left(1 - \frac{b^2}{3r_0^2} + \frac{a^2(4\cos^2\phi - 1)}{3r_0^2}\right)$$

where 2b is the height of the target and 2a is the length of the target. This correction is found to be negligible for our geometry.

The second correction is for the attenuation of both the incident beam and the elastically scattered gamma rays in the target. The actual number of counts in the peak, N_o, must be modified to obtain the number of counts which would be obtained if there were no absorption. This correction is[7]

$$N = N_o \frac{\sin\phi}{\mu\delta\omega}\left(1 - \exp\left(\frac{-\mu\delta\omega}{\sin\phi}\right)\right)$$

where μ is the attenuation coefficient[8,9], ω is the target thickness, ϕ is the angle the plane of the target makes whith the beam direction and $\delta = 1 + \frac{\sin\phi}{\sin(\theta - \phi)}$ where θ is the scattering angle.

RESULTS AND UNCERTAINTIES

One of the largest uncertainties in this experiment occurs in the measurement of the strength of the auxiliary source relative to the main source. The first auxiliary source (I) used has been previously measured[6] to have a strength of $(1.14 \pm .04) \times 10^{-7}$ times that of the main source. The ratio of the second auxiliary source (II) to the main source is $(1.47 \pm .05) \times 10^{-6}$.

All the targets and the auxiliary sources have dimensions of $16.5 \pm .05$ cm by $14.2 \pm .05$ cm. The mass of the first uranium target(1) used was $288.04 \pm .02$ gm; while the mass of the second uranium target (2) was $243.00 \pm .02$ gm. Thus the number of uranium atoms in the first target was $(0.73 \pm .01) \times 10^{24}$ and the number of uranium atoms in the second target was $(0.61 \pm .01) \times 10^{24}$. The uncertainty in the number of atoms is small, however a 2% uncertainty is introduced by the fact that spectroscopic analysis of the target reveals less than 2% by weight of impurities.[6]

The distance from the main source to the target was 148.7 ± 1.0 cm. In most cases this was the distance from the detector to the target. As a check at the smaller angles, a distance of twice this magnitude was used between the detector and the target.

Counting times were sufficiently long so that the counting statistics were better than 3%.

Another possible source of error was introduced by the electronic drift which caused the position of the peak to drift slightly. The peaks of each run were aligned and assigned the same channel number. The other channels were adjusted accordingly and the ratio of counts, n_a/n_b, was then calculated. This ratio and its uncertainty are listed in Table I.

The uncertainty in the scattering angle is the root mean square variation of the scattering angle over the target. In all cases this is less than or equal to $\pm$ 1°.

TABLE I. Summary of Present Results of the Differential Cross Section for Elastic Scattering of 1.33 MeV Gamma Rays from Uranium at 12°, 20°, 30°, 45° and 60°.

Scattering Angle (deg)	Target	Auxiliary Source	Geometric Arrangement	Absorption Correction	Counting Ratio (n_a/n_b)	Differential Cross Section (mb/sr)
12	No. 2	II	R = 2r	.582 ± .009	1.886 ± .036	203 ± 10
	No. 2	II	R = r	.615 ± .009	1.955 ± .039	200 ± 10
	No. 1	II	R = r	.537 ± .008	2.132 ± .043	206 ± 11
					Average:	203 ± 10
20	No. 2	II	R = 2r	.712 ± .011	.441 ± .015	38.8 ± 2.6
	No. 2	II	R = r	.738 ± .011	.496 ± .017	36.5 ± 2.0
	No. 1	II	R = 2r	.647 ± .010	.454 ± .016	37.2 ± 2.1
					Average:	37.5 ± 2.2
30	No. 2	I	R = r	.812 ± .012	2.236 ± .093	11.3 ± .6
45	No. 2	I	R = r	.863 ± .013	.368 ± .014	1.72 ± .09
60	No. 1	I	R = r	.870 ± .013	.108 ± .004	.430 ± .026

COMPARISON WITH OTHER EXPERIMENTS

The measurement of the elastic scattering cross section at 1.33 MeV for a uranium scatterer has also been performed by Bernstein and Mann[2] and Eberhard and Goldzahl[10]. However the uncertainties of their measurements were approximately 20% and hence considerably larger than ours.

Figure III gives a summary of all the experimental cross sections. The fact that the cross sections measured by the other groups were higher than ours at larger angles is most likely due to some inelastic events under the elastic scattering peak, since the resolution of their detector was much poorer than that of the present work.

Included in the experimental values in Figure III are those obtained with our experimental arrangement at larger angles by Schwandt.[6]

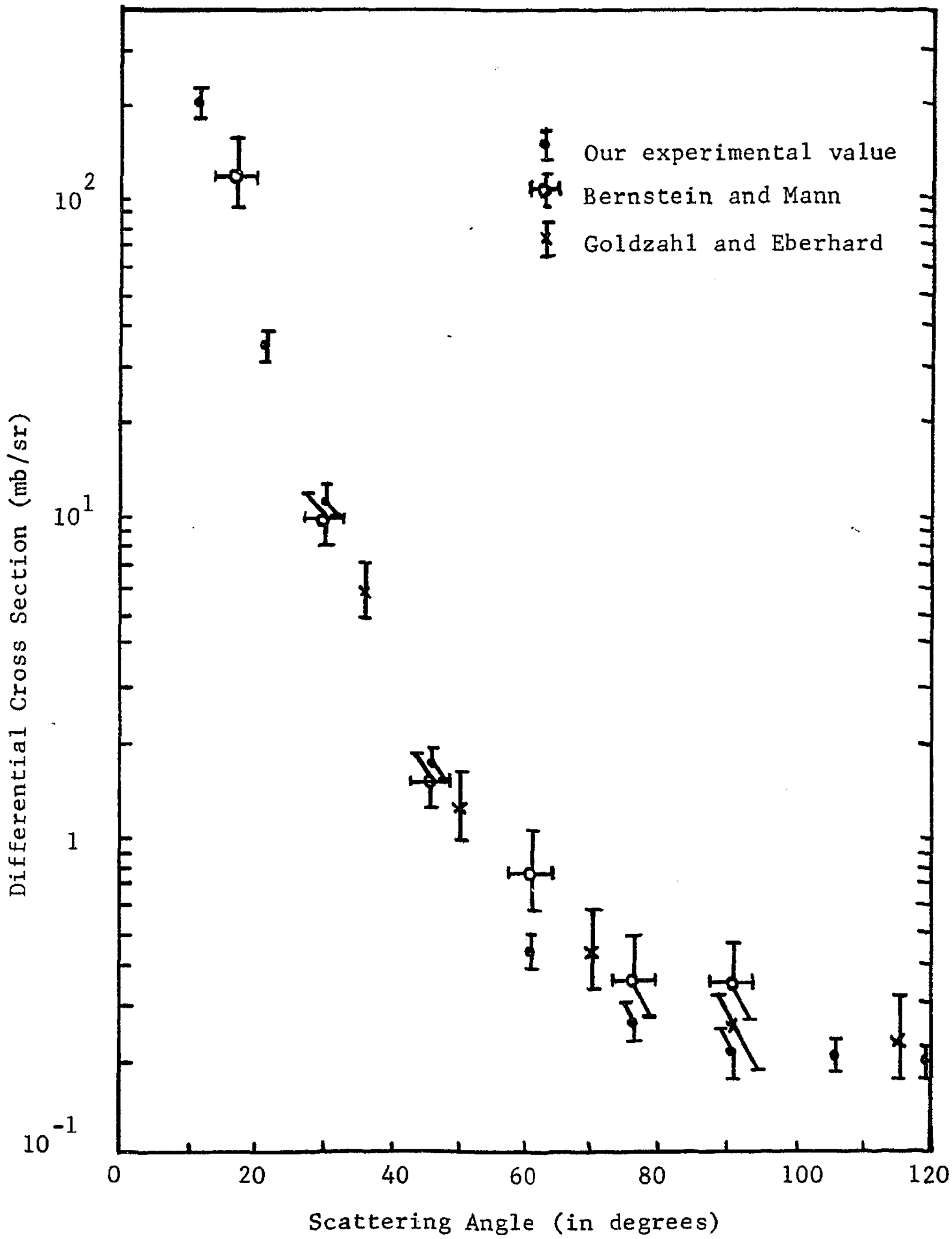

Figure III. Differential cross sections of other workers compared to our values.

THEORETICAL CALCULATIONS

The theoretical elastic scattering cross section is calculated from the Rayleigh, Thomson, and Delbruck scattering amplitudes. If this is to be compared with our experimental cross sections, these amplitudes must be known for a gamma ray energy of 1.33 MeV scattered from uranium.

Although there are several ways of expressing the polarization of the various scattering processes, the non-spin flip (NSF) and spin flip (SF) polarizations were chosen. All amplitudes were then expressed in this circular polarization.

The Thomson amplitudes are calculated exactly in Appendix II. The Delbruck amplitudes have been calculated by Ehlotsky and Sheppey[11] and can be easily adapted to any Z. These are calculated and listed in Appendix II.

The Rayleigh amplitudes have been calculated by Brown and Mayers[12] for a gamma ray energy of 1.31 MeV and a mercury scatterer. The difficulty in calculating the theoretical cross section arises in the extrapolation of these amplitudes to our particular energy and scatterer since the dependence on Z and E is unknown.

The simplest suggestion is to use the form factor approximation for the Rayleigh K-shell amplitude. The form factor is defined as the ratio of the radiation amplitude scattered by the actual electron distribution in an atom to that scattered by the actual electron distribution localized at a point[13]. The form factors for both K-shell and L-shell of mercury are calculated in Appendix I and illustrated in Figure IV. As can be seen, the agreement with the exact calculations is very poor.

However, the similarity in shapes of the form factor curves to those of the exact calculations suggests that a ratio of the form factors should be a fairly reliable method of extrapolation to a different Z.[12] Thus $a_R^K[92, 1.33, \theta] = \frac{F_K(92, 1.33, \theta)}{F_K(80, 1.31, \theta)} a_R^K[80, 1.31, \theta]$

These amplitudes are also calculated and listed in Appendix II, while the ratio of the form factors is calculated in Appendix I.

An attempt to determine the Z dependence of the cross section was made by Anand and Sood.[14] They found it does not vary strictly as Z^5 as is stated in most of the literature but that it varies as Z^n where n depends on the momentum transfer, Δq. An extrapolation of the Rayleigh amplitudes based on this Z dependence appears in Appendix II. Since their work was done with energies up to .662 MeV and scatterers of Z less than or equal to 82, there is some question as to the application of this dependence to higher energies and atomic numbers where Delbruck amplitudes are not negligible.

To compare the experimental results with theory and to determine the contribution of any one process to the differential cross section, it is convenient to calculate the theoretical cross sections for various combinations of the individual scattering processes. The program used to obtain the cross sections from the scattering amplitudes and the calculated values are found in Appendix III.

The following notation is used: R_1 denotes the extrapolation of

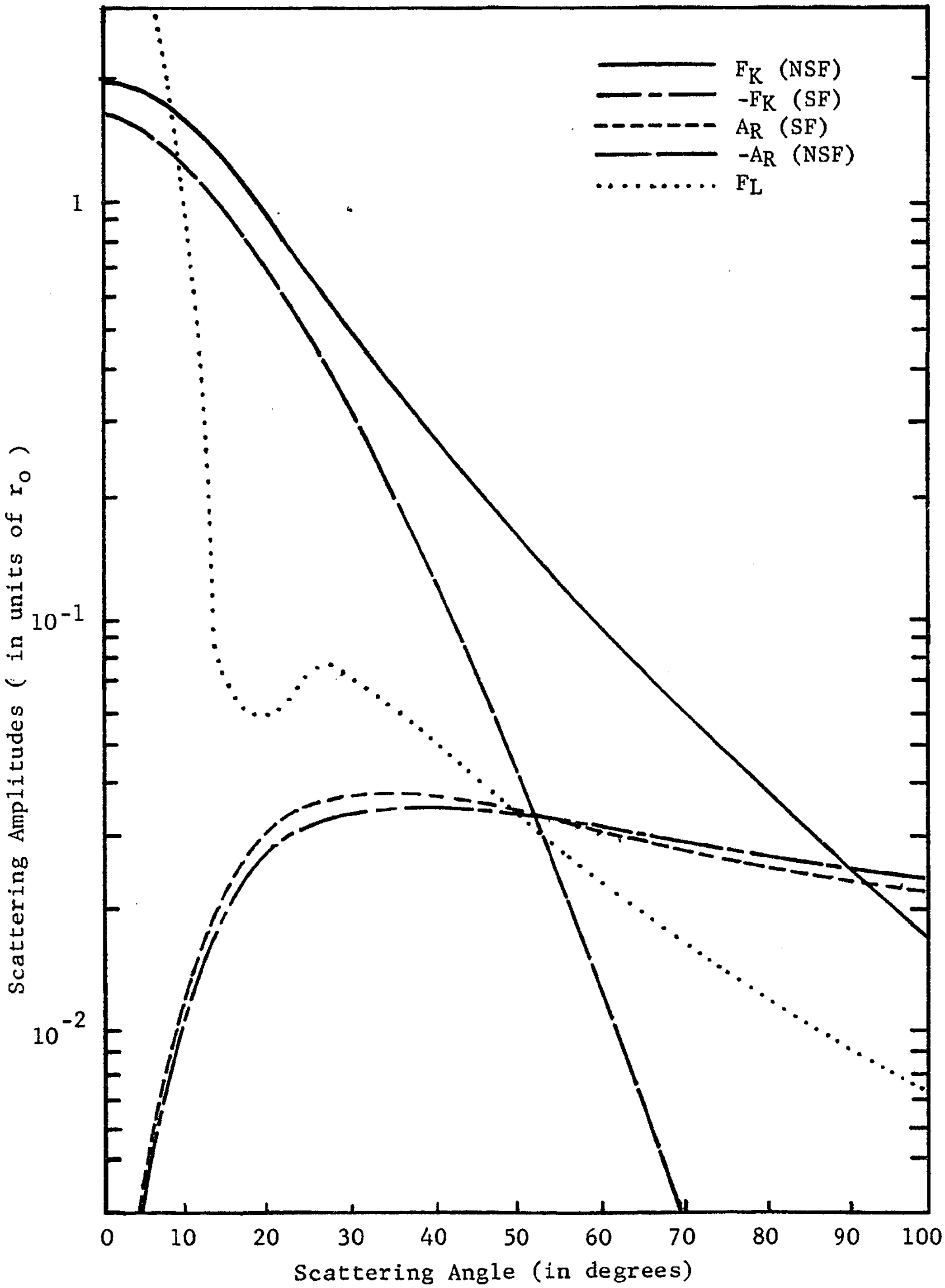

Figure IV. Comparison of form factor calculations with the exact Rayleigh amplitudes for Z = 80.

the Rayleigh amplitude obtained by a ratio of form factors, and R_2 denotes the extrapolation of the Rayleigh amplitude obtained using the Z dependence suggested by Anand and Sood.[14]

TABLE II

Summary of Notation for Theoretical Cross Sections

AMPLITUDES INCLUDED	R_1	R_2
Rayleigh (K-shell) and Thomson added coherently	CRSCA	CRSCG
Rayleigh (K-shell), Thomson and Delbruck added coherently	CRSCB	CRSCH
Rayleigh (K- and L-shell), Thomson, and Delbruck added coherently	CRSCC	CRSCI
Rayleigh (K-shell and L-shell (SF only)), Thomson, and Delbruck added coherently	CRSCD	CRSCJ
Rayleigh (K-and L-shell) and Thomson added coherently	CRSCE	CRSCK
Rayleigh (K- and L-shell) added incoherently to Thomson and Delbruck	CRSCF	CRSCL

COMPARISON WITH THEORETICAL CALCULATIONS

As can be seen from a study of Figure V, the difference in the theoretical cross section CRSCC due only to the difference in the method of extrapolating the Rayleigh amplitude is very large. This uncertainty due to extrapolation is much greater than the effect of Delbruck scattering.

Four possible values of the theoretical elastic cross section are illustrated in Figure VI. By comparing a theoretical cross section, CRSCC, composed of Thomson, Rayleigh (K- and L-shell), and Delbruck amplitudes to a theoretical cross section, CRSCE, composed of only Thomson and Rayleigh (K- and L-shell) amplitudes, one can see that the inclusion of Delbruck scattering varies the theoretical cross section slightly.

A further study of Figure VI shows the importance of including the Rayleigh L-shell contribution to both NSF and SF polarizations at smaller angles. The NSF Rayleigh L-shell amplitudes can be safely neglected only at large angles.

Part of the discrepancy in methods of extrapolation may be the assumption that the Z dependence determined by Anand and Sood[14] can be extended to higher energies. Figure VII illustrates the Z dependence of the cross section which they determined for energies of .280 MeV, .412 MeV, and .662 MeV. Also included in this figure is the Z dependence of the cross section for an energy of 1.33 MeV determined from our experiment using the same method which was employed by Anand

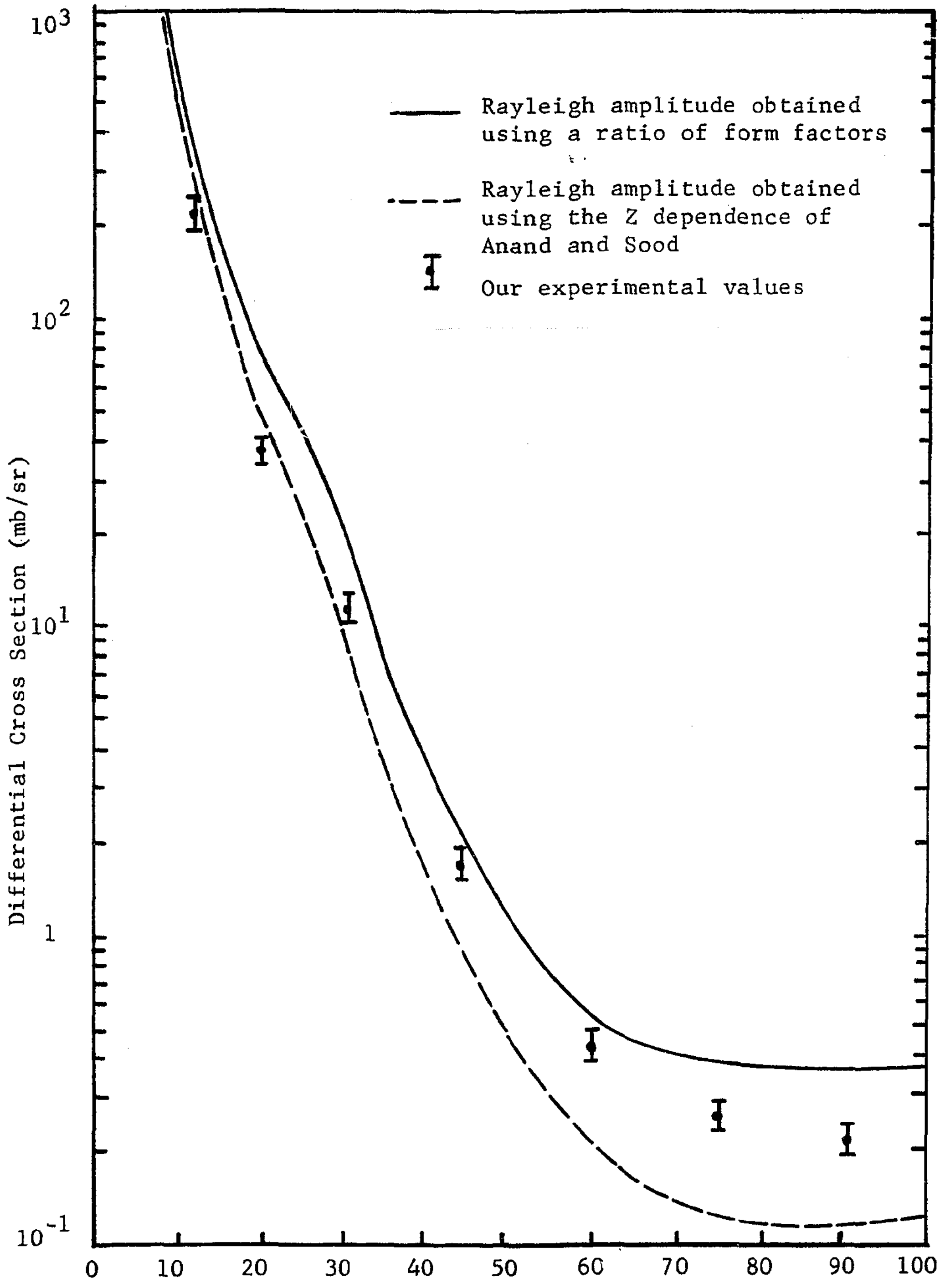

Figure V. Comparison of theoretical cross sections using two different methods of extrapolating the Rayleigh amplitudes.

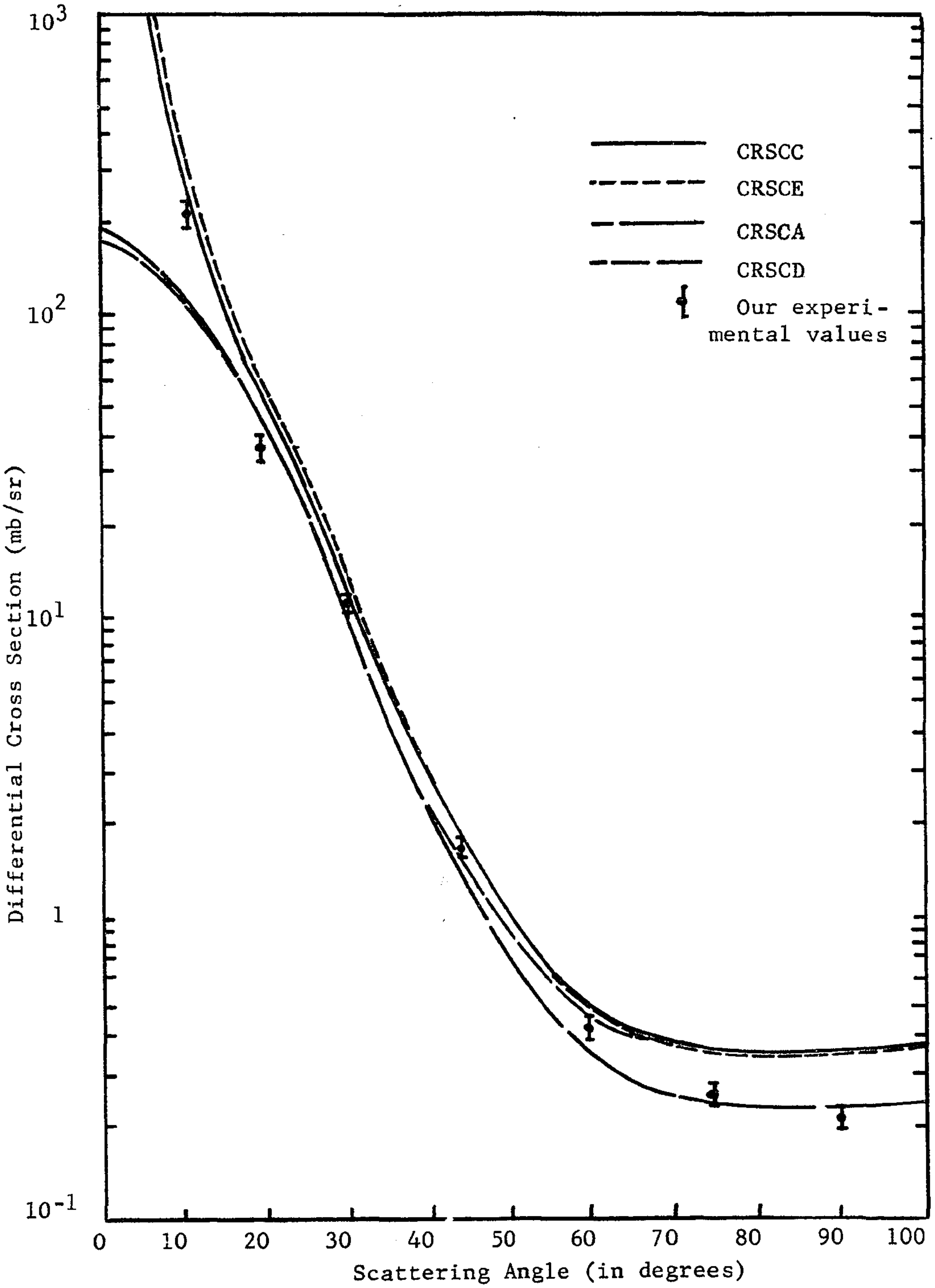

Figure VI. Various theoretical cross sections.

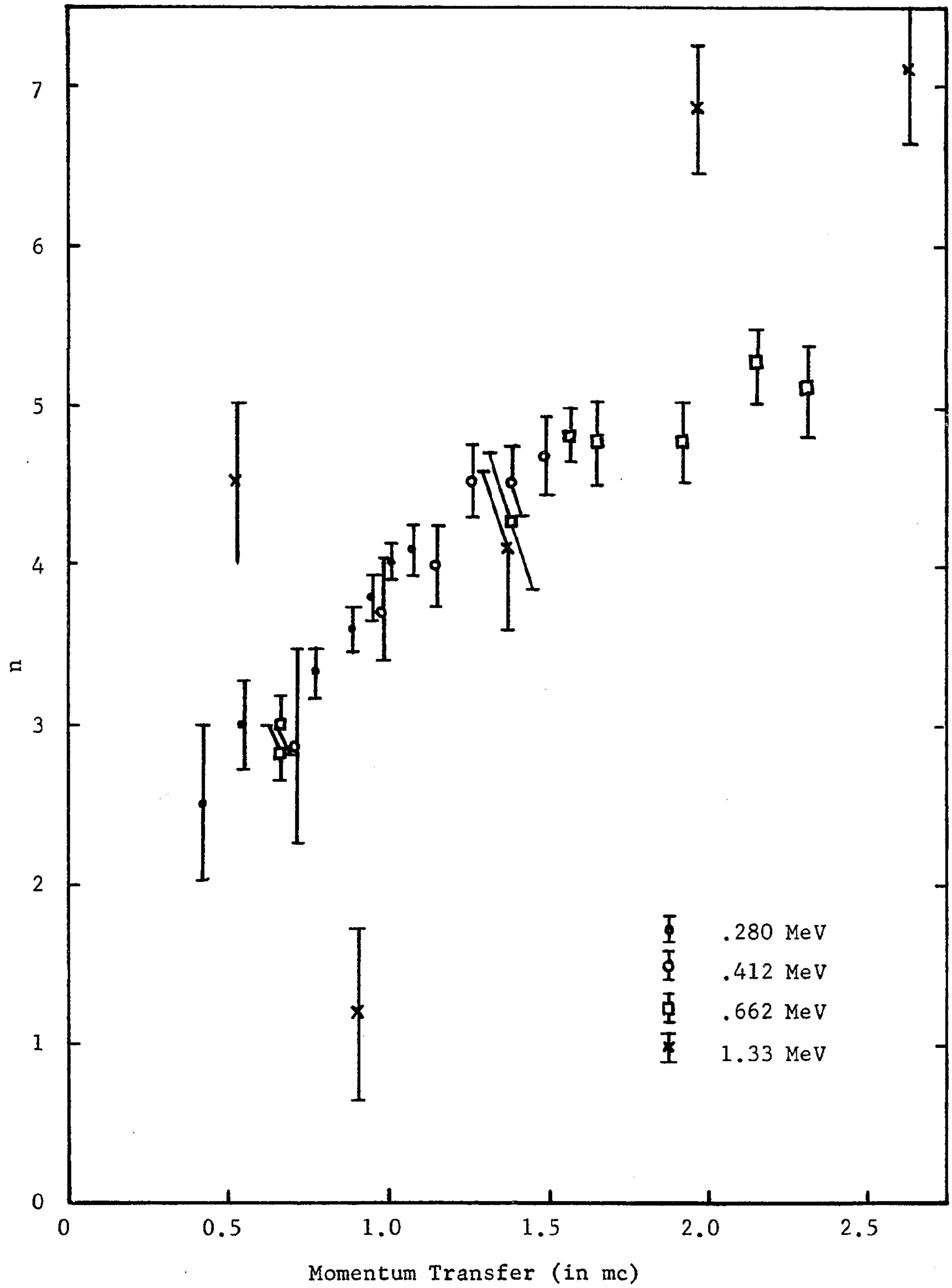

Figure VII. Variation of the index n with momentum transfer Δq.

and Sood.[14] As can be seen, the latter values are much higher than those used in the extrapolation of Rayleigh amplitudes by the second method.

The experimental data at 20° is lower than any theoretical calculation. This value as well as the value at 12° has been measured under a variety of experimental arrangements and consistent results have been obtained.

CONCLUSIONS

As can be observed from a study of Figure VI, no definite statement can be made about the existence of Delbruck scattering. The magnitude of the Delbruck amplitudes is much less than the uncertainty in the Rayleigh K-shell amplitudes. The Rayleigh L-shell amplitude, which is at least as large as the Delbruck amplitudes, has not been calculated exactly. Until this is done, one can simply observe that the experimental points coincide more closely to the curve which includes the Delbruck scattering amplitudes.

The Z dependence of the cross section determined by Anand and Sood[14], which was used as one method of extrapolating the Rayleigh amplitudes to a higher Z, could be invalid for energies greater than 1 MeV. As can be seen in Figure VII, the Z dependence of our experimental cross sections was considerably higher than the Z dependence which they determined.

A study of Figure VI also reveals that the inclusion of the Rayleigh L-shell contribution to both the spin flip and non-spin flip polarizations is important at smaller angles.

Thus a more accurate experimental value for the differential cross section at angles of 60°, 45°, 30°, 20° and 12° has been obtained. However the existence of Delbruck scattering cannot be proven experimentally until the theoretical calculations of Rayleigh K-shell and L-shell amplitudes have been done.

APPENDIX I

As mentioned previously, a calculation of the L-shell form factor is necessary to obtain an estimate of the Rayleigh L-shell amplitudes. This calculation of the L-shell form factor has been done by Woodward[15]. However since there were numerical errors in his work, the calculation has been redone and corrected in this appendix.

The densities given in Woodward's work are expressed as $\psi^*\psi$.

For a 1s electron $\psi^*\psi = \dfrac{1}{4\pi r^2}\,\dfrac{2^{2\nu+1}(Z\alpha m)^{2\nu+1}}{(2\nu)!}\,r^{2\nu}\,e^{-2Z\alpha m r}$.

The corresponding radial density ρ, which must satisfy $\int_0^\infty \rho\,dr = 1$ is $\rho_{1s} = \dfrac{2^{2\nu+1}(Z\alpha m)^{2\nu+1}}{(2\nu)!}\,r^{2\nu}\,e^{-2Z\alpha m r}$.

In general $\int_0^\infty r^a e^{-br} = a!\,b^{-a-1}$; $a > -1$, $\mathcal{R}(b) > 0$.

$$\therefore \int_0^\infty \rho_{1s}\,dr = \frac{(Z\alpha m)^{2\nu+1}(2^{2\nu+1})(2\nu)!}{(2\nu)!}(2Z\alpha m)^{-2\nu-1} = 1.$$

For the 2s electron

$$\psi\psi^* = \frac{1}{4\pi r^2}\,\frac{(2\nu+1)(Z\alpha m/\epsilon_1)^{2\nu+1}}{(2\nu)!\;2\epsilon_1(2\epsilon_1+1)}\,e^{-Z\alpha m r/\epsilon_1}\,r^{2\nu}$$

$$\times\left[1+\epsilon_1 - \frac{(1+\epsilon_1)Z\alpha m r}{(2\epsilon_1-1)\epsilon_1} + \frac{Z^2\alpha^2 m^2 r^2}{2(2\epsilon_1-1)^2\epsilon_1^2}\right].$$

where $\epsilon_1 = \sqrt{1+\frac{\nu}{2}}$

$$\int_0^\infty \rho_{2s}\,dr = \int_0^\infty \psi^*\psi\,4\pi r^2\,dr = \frac{2\nu+1\,(Z\alpha m/\epsilon_1)^{2\nu+1}}{2\epsilon_1(2\epsilon_1+1)(2\nu)!}\left(\frac{Z\alpha m}{\epsilon_1}\right)^{-2\nu-1}(2\nu)!$$

$$\times\left[1+\epsilon_1 - \frac{(1+\epsilon_1)(2\nu+1)}{(2\epsilon_1-1)} + \frac{(2\nu+1)(2\nu+2)}{2(2\epsilon_1-1)^2}\right]$$

$$= \frac{2\epsilon_1 - 1}{2\epsilon_1}\left[(1+\epsilon_1) - (1+\epsilon_1)(2\epsilon_1+1) + \frac{2\epsilon_1^2(2\epsilon_1+1)}{2\epsilon_1 - 1}\right] = 1$$

For the $2p_{1/2}$ electron

$$\psi^*\psi = \frac{1}{4\pi r^2}\frac{(2\nu+1)(Z\alpha m/\epsilon_1)^{2\nu+1}}{(2\nu)!\,2\epsilon_1(2\epsilon_1-1)} e^{-Z\alpha m r/\epsilon_1} r^{2\nu}$$

$$\times\left[(1-\epsilon_1) + \frac{(1-\epsilon_1)Z\alpha m r}{(2\epsilon_1+1)\epsilon_1} + \frac{Z^2\alpha^2 m^2 r^2}{2(2\epsilon_1+1)^2\epsilon_1^2}\right].$$

$$\int_0^\infty \rho_{2p_{1/2}} dr = \frac{(2\nu+1)(Z\alpha m/\epsilon_1)^{2\nu+1}}{(2\nu)!\,2\epsilon_1(2\epsilon_1-1)}(2\nu)!\left(\frac{Z\alpha m}{\epsilon_1}\right)^{-2\nu-1}$$

$$\times\left[(1-\epsilon_1) + \frac{(1+2\nu)(1-\epsilon_1)}{(2\epsilon_1+1)} + \frac{(2\nu+1)(2\nu+2)}{2(2\epsilon_1+1)^2}\right]$$

$$= \frac{4\epsilon_1^2 - 1}{2\epsilon_1(2\epsilon_1-1)}\left[1-\epsilon_1 + (1-\epsilon_1)(2\epsilon_1-1) + \frac{2\epsilon_1^2(2\epsilon_1^2-1)}{(2\epsilon_1+1)}\right] = 1$$

None of the $2p_{3/2}$ electrons have a spherically symmetric charge distribution; however, their average density, which is symmetric, is calculated. $\langle\psi^*\psi\rangle$ is quoted to be $\frac{1}{4\pi r^2}\frac{(Z\alpha m)^{4\epsilon_2+1}}{2(4\epsilon_2)!} r^{4\epsilon_2} e^{-Z\alpha m r}$ where $\epsilon_2 = \frac{\sqrt{4 - Z^2\alpha^2}}{2}$.

However, it can be shown directly from Dirac wave functions that this should be $\psi^*\psi = \frac{1}{4\pi r^2}\frac{(Z\alpha m)^{4\epsilon_2+1}}{(4\epsilon_2)!} r^{4\epsilon_2} e^{-Z\alpha m r}$.

Then $\int_0^\infty \rho_{2p_{3/2}} = \frac{(Z\alpha m)^{4\epsilon_2+1}}{(4\epsilon_2)!}(4\epsilon_2)!(Z\alpha m)^{-4\epsilon_2-1} = 1$

The form factors were calculated from the general formula

$$F = \int \psi^*\psi \exp(i\Delta q r\cos\theta)\, d\tau$$

where $\Delta q = \frac{2h\nu}{mc^2}\sin\frac{\theta'}{2} = \frac{2E_0}{.511}\sin\frac{\theta'}{2}$.

$$F = \int \rho/4\pi r^2 \exp(i\Delta q r\cos\theta)\, d\tau$$

$$= \frac{1}{4\pi}\int_0^{2\pi} d\phi \int_0^\infty\int_{-1}^1 \exp(i\Delta q r\cos\theta)\frac{\rho}{r^2} r^2 dr\, d(\cos\theta)$$

$$= \frac{1}{2}\int_0^\infty \left[\frac{\exp(i\Delta q r\cos\theta)}{i\Delta q r}\right|_{-1}^{1} \rho\, dr = \frac{1}{\Delta q}\int_0^\infty \rho\, \frac{\sin(\Delta q r)}{r}\, dr$$

$$F_{1S} = \frac{2^{2\nu+1}(Z\alpha m)^{2\nu+1}}{\Delta q\,(2\nu)!}\int_0^\infty r^{2\nu-1}\, e^{2Z\alpha m r}\,\sin(\Delta q r)\,dr$$

This and the following form factors are all integrated using the identity $\int_0^\infty e^{-px}\sin(qx)\,x^{R-1}\,dx = \frac{\Gamma(R)\sin(R\tan^{-1}q/p)}{(p+q)^{R/2}}$.

$$F_{1S} = \frac{Z\alpha m}{\nu\Delta q}\,\frac{\sin[2\nu\tan^{-1}(\Delta q/2Z\alpha m)]}{[1+(\Delta q/2Z\alpha m)^2]^\nu}$$

As noted in an earlier paper[12] the system of units used is one in which $\hbar = c = 1$ and momentum is measured in units of m. To compare this form factor to the formula used in the computer program, substitute $A = \frac{2E_0\sin\theta'/2}{.511\alpha Z} = \frac{\Delta q}{\alpha Z m c}$.

$$F_{2S} = \frac{\sin[2\nu\tan^{-1}(A/2)]}{\nu A[1+(A/2)^2]^\nu}$$

F_{2S} and $F_{2P_{1/2}}$ are grouped together. The average density is

$$\rho_{2S}+\rho_{2P_{1/2}} = \frac{2\nu+1\,(Z\alpha m/\epsilon_1)^{2\nu+1}}{2(2\nu)!\;2\epsilon_1}\, e^{-Z\alpha m r/\epsilon_1}\, r^{2\nu}$$
$$\times\left[\frac{2\epsilon_1}{4\epsilon_1^2-1} - \frac{Z\alpha m r}{\epsilon_1}\frac{(2\epsilon_1)}{(4\epsilon_1^2-1)} + \frac{(Z\alpha m r)^2}{2\epsilon_1^2}\frac{4\epsilon_1}{(4\epsilon_1^2-1)^2}\right]$$

Then

$$F_{2S}+F_{2P_{1/2}} = \frac{2\nu+1}{2(2\nu)!}\,\frac{(Z\alpha m/\epsilon_1)^{2\nu+1}}{\Delta q(4\epsilon_1^2-1)}$$
$$\times\left[\int_0^\infty e^{-Z\alpha m r/\epsilon_1}\, r^{2\nu-1}\,dr - \left(\frac{Z\alpha m}{\epsilon_1}\right)\int_0^\infty e^{-Z\alpha m r/\epsilon_1}\, r^{2\nu}\,dr + \left(\frac{Z\alpha m}{\epsilon_1}\right)^2\int_0^\infty e^{-Z\alpha m r/\epsilon_1}\, r^{2\nu+1}\,dr\right]$$

$$= \frac{Z\alpha m}{\epsilon_1\Delta q\left[1+\left(\frac{\epsilon_1\Delta q}{Z\alpha m}\right)^2\right]^\nu}\left[\frac{\sin 2\nu T}{2\nu} - \frac{\sin\overline{2\nu+1}\,T}{\left[1+\left(\frac{\epsilon_1\Delta q}{Z\alpha m}\right)^2\right]^{1/2}} + \frac{\sin\overline{2\nu+2}\,T}{\left[1+\left(\frac{\epsilon_1\Delta q}{Z\alpha m}\right)^2\right]}\right]$$

where $T = \tan^{-1}\left(\frac{\Delta q}{Z\alpha m/\epsilon_1}\right) = \tan^{-1}\epsilon_1 A.$

In terms of A

$$F_{2s} + F_{2p1/2} = \frac{1}{2\epsilon_1 A[1+\epsilon_1^2A^2]^\nu}\left[\frac{\sin 2\nu T}{2\nu} - \frac{\sin(2\nu+1)T}{[1+\epsilon_1^2A^2]^{1/2}} + \frac{\sin(2\nu+2)T}{[1+\epsilon_1^2A^2]}\right].$$

$$F_{2p3/2} = \frac{(Z\alpha m)^{4\epsilon_2+1}}{\Delta q(4\epsilon_2)!}\int_0^\infty r^{4\epsilon_2-1}e^{-Z\alpha m r}\sin(\Delta q r)\,dr$$

$$= \frac{(Z\alpha m)^{4\epsilon_2+1}}{4\epsilon_2\Delta q}\ \frac{\Gamma(4\epsilon_2)\sin(4\epsilon_2\tan^{-1}\Delta q/Z\alpha m)}{[1+(\Delta q/Z\alpha m)^2]^{2\epsilon_2}}$$

$$= \frac{Z\alpha m}{4\epsilon_2\Delta q}\ \frac{[\sin(4\epsilon_2\tan^{-1}(\Delta q/Z\alpha m))]}{[1+(\Delta q/Z\alpha m)^2]^{2\epsilon_2}}$$

This differs from Woodward's calculation[15] by a factor of 1/4.

$$F_{2p3/2} = \frac{1}{4\epsilon_2 A}\ \frac{\sin(4\epsilon_2\tan^{-1}A)}{[1+A^2]^{2\epsilon_2}}$$

Then the total form factor for the K-shell, F_K, is equal to $2F_{1s}$ and the total form factor for the L-shell is $F_L = 4(F_{2s}+F_{2p1/2}) + 4F_{2p3/2}$. Then the L-shell contribution is obtained by $a_R^L = (F_L/F_K)a_R^K$ where (F_L/F_K) is listed on pages 32, 33, and 34 for mercury, lead and uranium respectively.

As a check, the ratio at 0° will be computed:

$$\frac{F_L}{F_K} = \frac{4\left(\frac{\sin(4\epsilon_2\tan^{-1}A)}{4\epsilon_2[1+A^2]^{2\epsilon_2}}\right) + 4\left(\frac{1}{2\epsilon_1[1+\epsilon_1^2A^2]^\nu}\left[\frac{\sin 2\nu T}{2\nu} - \frac{\sin\overline{2\nu+1}T}{[1+\epsilon_1^2A^2]^{1/2}} + \frac{\sin\overline{2\nu+2}T}{[1+\epsilon_1^2A^2]}\right]\right)}{\frac{2}{\nu A}\ \frac{\sin[2\nu\tan^{-1}A/2]}{[1+(A/2)^2]^\nu}}.$$

If $\theta' = 0$, $\Delta q = 0$ and $T = 0$. Then the expression becomes

$$\frac{F_L}{F_K} = \frac{\sin(4\epsilon_2\tan^{-1}A)/\epsilon_2 + 2/\epsilon_1[(\sin 2\nu T/2\nu) + \sin\overline{2\nu+1}T + \sin\overline{2\nu+2}T]}{(2/\nu)(2\nu\tan^{-1}(A/2))}.$$

Applying l'Hopital's rule $\left(\frac{F_K}{F_L}\right)^{-1}$ as $\theta\to 0 = \frac{F_L'}{F_K'}$ as $\theta\to 0$.

$$\frac{F_L'}{F_K'} = \frac{\dfrac{\cos(4\epsilon_2 \tan^{-1} A}{\epsilon_2}\,\dfrac{4\epsilon_2}{(1+A^2)} + \dfrac{2}{\epsilon_1}\,\dfrac{\cos(2\nu \tan^{-1}\epsilon_1 A)2\nu\epsilon_1}{2\nu[1+\epsilon_1^2 A^2]}}{\dfrac{2}{\nu}(\cos(2\nu \tan^{-1}\dfrac{A}{2}))\,\dfrac{2\nu}{(1+(A/2)^2)}\,\dfrac{1}{2}}$$

$$+\frac{2}{\epsilon_1}\left(\frac{\dfrac{\cos[(2\nu+1)\tan^{-1}\epsilon_1 A](2\nu+1)\epsilon_1}{[1+(\epsilon_1 A)^2]} + \dfrac{\cos[(2\nu+2)\tan^{-1}\epsilon_1 A(2\nu+2)\epsilon_1]}{[1+(\epsilon_1 A)^2]}}{\dfrac{2}{\nu}(\cos(2\nu \tan^{-1}\dfrac{A}{2}))\,\dfrac{2\nu}{(1+(A/2)^2)}\,\dfrac{1}{2}}\right)$$

$$\lim_{A \to 0} = \frac{1}{2}(4 + 2[1 - (2\nu+1) + 2\nu + 2) = \frac{8}{2} = 4$$

A computer program which computes F_K, F_L, and the ratio F_K/F_L is found on page 31.

```
C      L SHELL CORRECTION FROM WOODWARD
401    READ 100,Z,ENOT,ANGS,ANGE,DANG,INDEX
100    FORMAT(F3.0,F8.3,3F7.2,I1)
       PUNCH 400
400    FORMAT(16H    Z       ENOT)
       PUNCH 300,Z,ENOT
300    FORMAT(F6.0,F11.3)
       PUNCH 500
500    FORMAT(14H ANGLE   RATIO)
       ALPHA =.0072972
       GAMMA = SQRTF(1.-((ALPHA*Z)**2))
       E1=SQRTF((1.+GAMMA)*.5)
       E2=.5*SQRTF(4.-((ALPHA*Z)**2))
403    ANGR=.017453*ANGS
       A=(2.*ENOT*SINF(.5*ANGR))/(.511*ALPHA*Z)
       D=GAMMA*A*((1.+((.5*A)**2))**GAMMA)
       FIS2=2.*SINF(2.*GAMMA*(ATANF(.5*A)))/D
       T=ATANF(E1*A)
       C=2./(E1*A*((1.+(E1*A)**2)**GAMMA))
       F2J14=C*((SINF(2.*GAMMA*T))/(2.*GAMMA)-SINF((2.*GAMMA+1.)*T)/
      1 ((1.+((E1*A)**2))**.5)+SINF((2.*GAMMA+2.)*T)/(1.+((E1*A)**2)))
       F2J34=   SINF(4.*E2*ATANF(A))/((E2*A)*(1.+(A**2))**(2.*E2))
       SUMF4=F2J14+F2J34
       RATIO=SUMF4/FIS2
       PUNCH 600,ANGS,FIS2,SUMF4,RATIO
600    FORMAT(F6.0,3E14.7)
       ANGS=ANGS+DANG
       DIFF=ANGE-ANGS
       IF(DIFF)402,402,403
402    IF(INDEX)404,401,404
404    CALL EXIT
       END
```

TABLE III

ANGLE	F(K)	F(L)	RATIO
5.	1.8857714E+00	4.1085818E+00	2.1787273E+00
10.	1.6008767E+00	7.0837870E-01	4.4249422E-01
15.	1.2611805E+00	7.4910020E-02	5.9396747E-02
20.	9.5301706E-01	5.8309274E-02	6.1183872E-02
25.	7.0900879E-01	7.3946814E-02	1.0429604E-01
30.	5.2817987E-01	7.1623608E-02	1.3560457E-01
35.	3.9778174E-01	6.1538561E-02	1.5470433E-01
40.	3.0428922E-01	5.0557074E-02	1.6614809E-01
45.	2.3686746E-01	4.1011732E-02	1.7314211E-01
50.	1.8767760E-01	3.3321087E-02	1.7754429E-01
55.	1.5127440E-01	2.7289880E-02	1.8039985E-01
60.	1.2392464E-01	2.2592028E-02	1.8230456E-01
65.	1.0306750E-01	1.8923887E-02	1.8360673E-01
70.	8.6933059E-02	1.6040558E-02	1.8451620E-01
75.	7.4284073E-02	1.3754676E-02	1.8516319E-01
80.	6.4244752E-02	1.1925788E-02	1.8563053E-01
85.	5.6186573E-02	1.0449159E-02	1.8597252E-01
90.	4.9652522E-02	9.2465639E-03	1.8622546E-01
95.	4.4305946E-02	8.2592497E-03	1.8641402E-01
100.	3.9895736E-02	7.4427720E-03	1.8655557E-01
105.	3.6232439E-02	6.7632310E-03	1.8666231E-01
110.	3.3171556E-02	6.1945571E-03	1.8674303E-01
115.	3.0601747E-02	5.7165352E-03	1.8680421E-01
120.	2.8436515E-02	5.3133761E-03	1.8685046E-01
125.	2.6608060E-02	4.9726598E-03	1.8688547E-01
130.	2.5062906E-02	4.6845538E-03	1.8691183E-01
135.	2.3758653E-02	4.4412428E-03	1.8693159E-01
140.	2.2661533E-02	4.2364899E-03	1.8694630E-01
145.	2.1744628E-02	4.0653141E-03	1.8695716E-01
150.	2.0986500E-02	3.9237439E-03	1.8696513E-01
155.	2.0370157E-02	3.8086252E-03	1.8697083E-01
160.	1.9882293E-02	3.7174902E-03	1.8697492E-01
165.	1.9512700E-02	3.6484389E-03	1.8697765E-01
170.	1.9253832E-02	3.6000705E-03	1.8697942E-01
175.	1.9100507E-02	3.5714209E-03	1.8698042E-01

TABLE IV

ANGLE	F(K)	F(L)	RATIO
5.	1.8925130E+00	4.2664575E+00	2.2543874E+00
10.	1.6218379E+00	8.1299208E-01	5.0127825E-01
15.	1.2938195E+00	9.5057190E-02	7.3470209E-02
20.	9.9060085E-01	6.0098950E-02	6.0669188E-02
25.	7.4605124E-01	7.6084150E-02	1.0198247E-01
30.	5.6181081E-01	7.5493588E-02	1.3437546E-01
35.	4.2706116E-01	6.6100535E-02	1.5478002E-01
40.	3.2929053E-01	5.5073046E-02	1.6724758E-01
45.	2.5807455E-01	4.5157113E-02	1.7497700E-01
50.	2.0567650E-01	3.7001034E-02	1.7989918E-01
55.	1.6662065E-01	3.0512458E-02	1.8312530E-01
60.	1.3709788E-01	2.5404000E-02	1.8529827E-01
65.	1.1446449E-01	2.1381765E-02	1.8679823E-01
70.	9.6875473E-02	1.8198665E-02	1.8785626E-01
75.	8.3030695E-02	1.5660973E-02	1.8861666E-01
80.	7.2003338E-02	1.3621020E-02	1.8917206E-01
85.	6.3124338E-02	1.1967325E-02	1.8958337E-01
90.	5.5904674E-02	1.0615822E-02	1.8989149E-01
95.	4.9982370E-02	9.5028786E-03	1.9012460E-01
100.	4.5086398E-02	8.5800498E-03	1.9030240E-01
105.	4.1011500E-02	7.8101847E-03	1.9043889E-01
110.	3.7600608E-02	7.1645787E-03	1.9054422E-01
115.	3.4732363E-02	6.6208867E-03	1.9062586E-01
120.	3.2312197E-02	6.1615893E-03	1.9068927E-01
125.	3.0265847E-02	5.7728657E-03	1.9073861E-01
130.	2.8534585E-02	5.4437430E-03	1.9077701E-01
135.	2.7071760E-02	5.1654790E-03	1.9080691E-01
140.	2.5840158E-02	4.9310795E-03	1.9083008E-01
145.	2.4810066E-02	4.7349505E-03	1.9084796E-01
150.	2.3957782E-02	4.5726232E-03	1.9086170E-01
155.	2.3264497E-02	4.4405445E-03	1.9087214E-01
160.	2.2715487E-02	4.3359300E-03	1.9087990E-01
165.	2.2299409E-02	4.2566329E-03	1.9088545E-01
170.	2.2007905E-02	4.2010717E-03	1.9088921E-01
175.	2.1835221E-02	4.1681544E-03	1.9089133E-01

TABLE V

ANGLE	F(K)	F(L)	RATIO
5.	1.9204047E+00	4.9780448E+00	2.5921852E+00
10.	1.7117874E+00	1.4207436E+00	8.2997666E-01
15.	1.4409945E+00	2.7024016E-01	1.8753725E-01
20.	1.1693042E+00	9.2112280E-02	7.8775292E-02
25.	9.3131349E-01	9.0757070E-02	9.7450612E-02
30.	7.3781976E-01	9.5950000E-02	1.3004531E-01
35.	5.8648423E-01	9.1182120E-02	1.5547241E-01
40.	4.7014786E-01	8.1298233E-02	1.7292056E-01
45.	3.8111827E-01	7.0363085E-02	1.8462270E-01
50.	3.1278898E-01	6.0223616E-02	1.9253752E-01
55.	2.5997900E-01	5.1473769E-02	1.9799202E-01
60.	2.1879059E-01	4.4159104E-02	2.0183273E-01
65.	1.8634338E-01	3.8125006E-02	2.0459544E-01
70.	1.6052086E-01	3.3167267E-02	2.0662278E-01
75.	1.3976545E-01	2.9090468E-02	2.0813776E-01
80.	1.2292490E-01	2.5726772E-02	2.0928853E-01
85.	1.0914038E-01	2.2938624E-02	2.1017540E-01
90.	9.7766269E-02	2.0615760E-02	2.1086781E-01
95.	8.8312835E-02	1.8670618E-02	2.1141454E-01
100.	8.0405175E-02	1.7033882E-02	2.1185056E-01
105.	7.3753788E-02	1.5650653E-02	2.1220134E-01
110.	6.8133178E-02	1.4477323E-02	2.1248565E-01
115.	6.3366348E-02	1.3479131E-02	2.1271749E-01
120.	5.9313368E-02	1.2628260E-02	2.1290748E-01
125.	5.5862922E-02	1.1902366E-02	2.1306379E-01
130.	5.2925941E-02	1.1283420E-02	2.1319261E-01
135.	5.0430926E-02	1.0756859E-02	2.1329885E-01
140.	4.8320298E-02	1.0310892E-02	2.1338634E-01
145.	4.6547669E-02	9.9359759E-03	2.1345807E-01
150.	4.5075801E-02	9.6244181E-03	2.1351629E-01
155.	4.3874925E-02	9.3700564E-03	2.1356290E-01
160.	4.2921587E-02	9.1680210E-03	2.1359930E-01
165.	4.2197668E-02	9.0145433E-03	2.1362657E-01
170.	4.1689744E-02	8.9068294E-03	2.1364557E-01
175.	4.1388561E-02	8.8429458E-03	2.1365675E-01

APPENDIX II

This appendix lists the amplitudes of the various elastic scattering processes. All amplitudes are given in units of r_o, the classical electron radius.

The program listed on pages 38 and 39 was used to obtain the tables of scattering amplitudes.

The Thomson amplitudes have been calculated from the following equations:

$$a_T(NSF) = -\frac{(Ze)^2}{M_n}\,\frac{\cos\theta + 1}{2}$$

$$a_T(SF) = +\frac{(Ze)^2}{M_n}\,\frac{-\cos\theta + 1}{2}$$

where M_n is the mass of the nucleus. $\frac{(Ze)^2}{M_n}$ can be written as $r_o \frac{M_e c^2}{e^2}\frac{(Ze)^2}{M_n}$ or $r_o \frac{M_e}{M_n} Z^2 c^2$. This can be expressed as $r_o Z^2 \left(\frac{M_e}{M_p} \Big/ \frac{M_n}{M_p}\right)$ where $\frac{M_e}{M_p}$ has a value of 5.446×10^{-4}. Therefore the Thomson amplitudes may be written as

$$a_T(NSF) = (-2.723 \times 10^{-4})\, r_o \frac{Z^2}{\frac{M_n}{M_p}} (\cos\theta + 1)$$

$$a_T(SF) = (2.723 \times 10^{-4})\, r_o \frac{Z^2}{\frac{M_n}{M_p}} (-\cos\theta + 1)$$

where M_n / M_p = 205.55 for lead and 236.15 for uranium. The program uses the last two equations to calculate the Thomson amplitudes. Tables VI and XI give these amplitudes for lead and uranium respectively at an energy of 1.33 MeV.

Ehlotsky and Sheppey[11] have listed the parallel ($\parallel$) and perpendiculare ($\perp$) components of the Delbruck amplitudes for scattering angles less than or equal to 120°. These were converted to NSF and SF polarizations by using equations $a(NSF) = \frac{1}{2}[a_{\parallel} + a_{\perp}]$

for both real and imaginary amplitudes. To obtain amplitudes in units of r_o, their amplitudes had to be multiplied by $(\alpha Z)^2$ where α, the fine structure constant, has a value of 7.2971×10^{-3}. These values were then plotted as a function of the angle and the values at 5° increments were read from the graph. These graphs were extrapolated to obtain amplitudes to a scattering angle of 135°. Table VII and XII give these amplitudes for lead and uranium respectively.

Brown and Mayers[12] have made numerical calculations of the Rayleigh K-shell amplitudes for a mercury scatterer and an energy of 1.31 MeV. These were plotted (with all signs changed[16]) as a function of angle and the values at 5° increments were obtained from the graph.

These values then had to be extrapolated for lead and uranium scatterers and an energy of 1.33 MeV. Two methods were used. In the first method, the extrapolation was done using the form factor amplitudes as follows: $a_R[Z=92, 1.33\ \text{MeV}] = \dfrac{F(Z=92, 1.33\ \text{MeV})}{F(Z=80, 1.31\ \text{MeV})}\, a_R[Z=80, 1.31\ \text{MeV}]$

In the second method, the mercury amplitudes were first adjusted from 1.31 MeV to 1.33 MeV by using form factors:

$$a_R[Z=80, 1.33\ \text{MeV}] = \frac{F(Z=80, 1.33\ \text{MeV})}{F(Z=80, 1.31\ \text{MeV})}\, a_R[Z=80, 1.31\ \text{MeV}]$$

Then, following the suggestion of Anand and Sood[14], for a particular θ

$$a_T(\text{NSF})(Z) + a_R(\text{NSF})(Z) = \left[a_T(\text{NSF})(80) + a_R(Z=80, 1.33\ \text{MeV})\right]\left(\frac{Z}{80}\right)^{n/2}$$

where n is a function of the momentum change of the photon due to the the scattering. This momentum transfer is given by:

$$q = 2\left(\frac{h\nu}{mc^2}\right)\sin\left(\frac{\theta}{2}\right) = 2\left(\frac{E_0}{mc^2}\right)\sin\frac{\theta}{2} = 2\,\frac{E_0}{.511}\sin\frac{\theta}{2}$$

with E_o in MeV. This value was used to obtain the corresponding n from the paper by Anand and Sood[14]. The Rayleigh K-shell amplitudes obtained by using the first method of extrapolation (ARNSF, ARSF, BRNSF, BRSF) are given in Tables VIII and XIII for lead and uranium respectively, while those amplitudes obtained with the second method of extrapolation (CRNSF, CRSF, DRNSF, DRSF) are given in Tables IX and XIV for lead and uranium respectively.

The Rayleigh L-shell amplitudes were obtained from the Rayleigh K-shell amplitudes in the following manner:

$$a_R^L = a_R^K\left(\frac{F_L}{F_K}\right)$$

The form factors are discussed in Appendix I. The L-shell amplitudes listed in Tables XV and XX were obtained from the Rayleigh K-shell amplitudes ex rapolated by the first method.

```
      DIMENSION ADSF(37),BDNSF(37),BDSF(37),ATSF(37),ATNSF(37)
      DIMENSION ARNSF(37),ARSF(37),BRNSF(37),BRSF(37),ADNSF(37),
     1 ANGR(37),RN(37),RATIO(37),CRNSF(37),CRSF(37),DRNSF(37),
     1 DRSF(37),ANGS(38)
      READ 20,Z,RAT
20    FORMAT(F4.0,F9.5)
      READ 10,(ARNSF(I),I=1,37)
      READ 10,(ARSF(I),I=1,37)
      READ 10,(BRNSF(I),I=1,37)
      READ 10,(BRSF(I),I=1,37)
      READ 10,(RN(I),I=1,37)
      READ 10,(RATIO(I),I=1,37)
10    FORMAT(11F7.4)
      ANGS(1)=0.
      DO 30 I=1,37
      ANGR(I)=.017543*ANGS(I)
      ATNSF(I)=(-.0002723)*(Z**2)*(COSF(ANGR(I))+1.)/RAT
      ATSF(I)=(-.0002723)*(Z**2)*(COSF(ANGR(I))-1.)/RAT
      CRNSF(I)=(ATNSF(I)+ARNSF(I)*RATIO(I))*(Z/80.)**(RN(I)/2.)
      CRSF(I)=(ATSF(I)+ARSF(I)*RATIO(I))*(Z/80.)**(RN(I)/2.)
      DRNSF(I)=(BRNSF(I)*RATIO(I))*(Z/80.)**(RN(I)/2.)
      DRSF(I)=(BRSF(I)*RATIO(I))*(Z/80.)**(RN(I)/2.)
30    ANGS(I+1)=ANGS(I)+5.
90    READ 20,Z,RAT
      READ 10,(ARNSF(I),I=1,37)
      READ 10,(ARSF(I),I=1,37)
      READ 10,(BRNSF(I),I=1,37)
      READ 10,(BRSF(I),I=1,37)
      READ 10,(ADNSF(I),I=1,37)
      READ 10,(ADSF(I),I=1,37)
      READ 10,(BDNSF(I),I=1,37)
      READ 10,(BDSF(I),I=1,37)
      READ 10,(RATIO(I),I=1,37)
      ANGS(1)=0.
      DO 40 I=1,37
```

```
      ANGR(I)=.017543*ANGS(I)
      ATNSF(I)=(-.0002723)*(Z**2)*(COSF(ANGR(I))+1.)/RAT
      ATSF(I)=(-.0002723)*(Z**2)*(COSF(ANGR(I))-1.)/RAT
      CRNSF(I)=CRNSF(I)-ATNSF(I)
      CRSF(I)=CRSF(I)-ATSF(I)
      PUNCH 11,ANGS(I),ATNSF(I),ATSF(I)
11    FORMAT(F6.0,2F11.4)
40    ANGS(I+1)=ANGS(I)+5.
      DO 50 I=1,37
50    PUNCH 12,ANGS(I),ADNSF(I),ADSF(I),BDNSF(I),BDSF(I)
12    FORMAT(F6.0,4F11.4)
      DO 60 I=1,37
60    PUNCH 12,ANGS(I),ARNSF(I),ARSF(I),BRNSF(I),BRSF(I)
      DO 70 I=1,37
70    PUNCH 12, ANGS(I),CRNSF(I),CRSF(I),DRNSF(I),DRSF(I)
      DO 80 I=1,37
      ARNSF(I)=ARNSF(I)*RATIO(I)
      ARSF(I)=ARSF(I)*RATIO(I)
      BRNSF(I)=BRNSF(I)*RATIO(I)
      BRSF(I)=BRSF(I)*RATIO(I)
80    PUNCH 12,ANGS(I),ARNSF(I),ARSF(I),BRNSF(I),BRSF(I)
      PUNCH  10,(CRNSF(I),I=1,37)
      PUNCH 10,(CRSF(I),I=1,37)
      PUNCH 10,(DRNSF(I),I=1,37)
      PUNCH 10,(DRSF(I),I=1,37)
      CALL EXIT
      END
```

TABLE VI

ANGLE	ATNSF	ATSF
0.	-.0178	0.0000
5.	-.0177	0.0000
10.	-.0176	.0001
15.	-.0175	.0003
20.	-.0172	.0005
25.	-.0169	.0008
30.	-.0166	.0012
35.	-.0161	.0016
40.	-.0157	.0021
45.	-.0151	.0026
50.	-.0146	.0032
55.	-.0139	.0038
60.	-.0133	.0044
65.	-.0126	.0051
70.	-.0119	.0059
75.	-.0111	.0066
80.	-.0103	.0074
85.	-.0096	.0081
90.	-.0088	.0089
95.	-.0080	.0097
100.	-.0072	.0105
105.	-.0065	.0112
110.	-.0057	.0120
115.	-.0050	.0127
120.	-.0043	.0134
125.	-.0037	.0140
130.	-.0031	.0147
135.	-.0025	.0152
140.	-.0020	.0158
145.	-.0015	.0162
150.	-.0011	.0166
155.	-.0007	.0170
160.	-.0004	.0173
165.	-.0002	.0175
170.	-.0001	.0177
175.	0.0000	.0177
180.	0.0000	.0178

TABLE VII

ANGLE	ADNSF	ADSF	BDNSF	BDSF
0.	.0856	0.0000	0.0000	0.0000
5.	.0415	.0020	.0160	.0001
10.	.0234	.0027	.0198	.0002
15.	.0173	.0028	.0194	.0003
20.	.0132	.0029	.0179	.0004
25.	.0103	.0028	.0163	.0007
30.	.0081	.0027	.0149	.0009
35.	.0066	.0024	.0133	.0012
40.	.0053	.0023	.0117	.0015
45.	.0042	.0023	.0104	.0018
50.	.0034	.0022	.0089	.0021
55.	.0027	.0021	.0077	.0024
60.	.0022	.0020	.0066	.0027
65.	.0018	.0020	.0056	.0031
70.	.0015	.0019	.0048	.0035
75.	.0013	.0018	.0039	.0038
80.	.0011	.0018	.0033	.0041
85.	.0009	.0018	.0026	.0043
90.	.0007	.0017	.0022	.0046
95.	.0006	.0017	.0018	.0048
100.	.0005	.0017	.0015	.0050
105.	.0004	.0017	.0012	.0052
110.	.0003	.0017	.0010	.0054
115.	.0002	.0016	.0007	.0056
120.	.0002	.0016	.0005	.0057
125.	.0002	.0016	.0004	.0058
130.	.0001	.0016	.0003	.0060
135.	.0001	.0016	.0001	.0061

TABLE VIII

ANGLE	ARNSF	ARSF	BRNSF	BRSF
0.	-1.6989	0.0000	.0474	0.0000
5.	-1.4424	.0078	.0469	-.0023
10.	-1.1197	.0157	.0410	-.0028
15.	-.9821	.0236	.0319	-.0041
20.	-.7298	.0307	.0231	-.0064
25.	-.5089	.0366	.0177	-.0079
30.	-.3006	.0387	.0138	-.0081
35.	-.1770	.0385	.0118	-.0080
40.	-.1130	.0376	.0103	-.0078
45.	-.0780	.0359	.0090	-.0072
50.	-.0528	.0343	.0084	-.0066
55.	-.0318	.0326	.0078	-.0059
60.	-.0141	.0312	.0074	-.0054
65.	-.0078	.0297	.0069	-.0049
70.	-.0021	.0284	.0064	-.0044
75.	.0027	.0272	.0064	-.0043
80.	.0055	.0264	.0058	-.0037
85.	.0064	.0256	.0054	-.0034
90.	.0067	.0252	.0047	-.0032
95.	.0066	.0249	.0045	-.0031
100.	.0063	.0246	.0041	-.0030
105.	.0057	.0243	.0037	-.0029
110.	.0052	.0241	.0033	-.0028
115.	.0047	.0238	.0028	-.0027
120.	.0041	.0234	.0025	-.0026
125.	.0036	.0236	.0020	-.0026
130.	.0031	.0236	.0015	-.0026
135.	.0025	.0238	.0011	-.0026
140.	.0020	.0233	.0010	-.0025
145.	.0015	.0232	.0009	-.0025
150.	.0012	.0237	.0008	-.0024
155.	.0011	.0231	.0007	-.0024
160.	.0010	.0229	.0005	-.0024
165.	.0010	.0229	.0004	-.0022
170.	.0009	.0228	.0003	-.0024
175.	.0008	.0226	.0002	-.0024
180.	0.0000	.0226	0.0000	-.0025

TABLE IX

ANGLE	CRNSF	CRSF	DRNSF	DRSF
0.	-1.6955	0.0000	.0473	0.0000
5.	-1.4279	.0077	.0464	-.0022
10.	-1.1675	.0153	.0399	-.0027
15.	-.9400	.0225	.0305	-.0039
20.	-.6857	.0289	.0216	-.0059
25.	-.4702	.0338	.0163	-.0072
30.	-.2737	.0352	.0125	-.0073
35.	-.1591	.0346	.0106	-.0072
40.	-.1005	.0334	.0091	-.0069
45.	-.0685	.0316	.0079	-.0063
50.	-.0461	.0300	.0074	-.0057
55.	-.0275	.0283	.0068	-.0051
60.	-.0120	.0270	.0064	-.0047
65.	-.0065	.0255	.0059	-.0042
70.	-.0016	.0242	.0055	-.0038
75.	.0024	.0232	.0055	-.0036
80.	.0048	.0225	.0049	-.0031
85.	.0056	.0217	.0046	-.0028
90.	.0058	.0212	.0040	-.0026
95.	.0056	.0209	.0038	-.0025
100.	.0054	.0207	.0034	-.0024
105.	.0049	.0204	.0031	-.0024
110.	.0045	.0202	.0027	-.0023
115.	.0040	.0199	.0023	-.0022
120.	.0035	.0195	.0021	-.0022
125.	.0031	.0196	.0016	-.0022
130.	.0026	.0195	.0012	-.0022
135.	.0021	.0197	.0009	-.0022
140.	.0016	.0192	.0008	-.0021
145.	.0012	.0191	.0007	-.0021
150.	.0010	.0196	.0006	-.0020
155.	.0009	.0190	.0005	-.0020
160.	.0008	.0188	.0004	-.0020
165.	.0008	.0188	.0003	-.0018
170.	.0007	.0187	.0002	-.0020
175.	.0006	.0187	.0001	-.0020
180.	0.0000	.0185	0.0000	-.0021

TABLE X

ANGLE	ARLNSF	ARLSF	BRLNSF	BRLSF
0.	-6.7956	0.0000	.1896	0.0000
5.	-3.2517	.0175	.1057	-.0051
10.	-.5613	.0078	.0205	-.0014
15.	-.0721	.0017	.0023	-.0003
20.	-.0442	.0018	.0014	-.0003
25.	-.0518	.0037	.0018	-.0008
30.	-.0404	.0052	.0018	-.0010
35.	-.0273	.0059	.0018	-.0012
40.	-.0188	.0062	.0017	-.0013
45.	-.0136	.0062	.0015	-.0012
50.	-.0094	.0061	.0015	-.0011
55.	-.0058	.0059	.0014	-.0010
60.	-.0026	.0057	.0013	-.0010
65.	-.0014	.0055	.0012	-.0009
70.	-.0003	.0053	.0012	-.0008
75.	.0005	.0051	.0012	-.0008
80.	.0010	.0049	.0010	-.0007
85.	.0012	.0048	.0010	-.0006
90.	.0012	.0047	.0008	-.0006
95.	.0012	.0047	.0008	-.0005
100.	.0011	.0046	.0007	-.0005
105.	.0010	.0046	.0007	-.0005
110.	.0009	.0045	.0006	-.0005
115.	.0008	.0045	.0005	-.0005
120.	.0007	.0044	.0004	-.0004
125.	.0006	.0045	.0003	-.0004
130.	.0005	.0045	.0002	-.0004
135.	.0004	.0045	.0002	-.0004
140.	.0003	.0044	.0001	-.0004
145.	.0002	.0044	.0001	-.0004
150.	.0002	.0045	.0001	-.0004
155.	.0002	.0044	.0001	-.0004
160.	.0001	.0043	0.0000	-.0004
165.	.0001	.0043	0.0000	-.0004
170.	.0001	.0043	0.0000	-.0004
175.	.0001	.0043	0.0000	-.0004
180.	0.0000	.0043	0.0000	-.0004

TABLE XI

ANGLE	ATNSF	ATSF
0.	-.0195	0.0000
5.	-.0194	0.0000
10.	-.0193	.0001
15.	-.0191	.0003
20.	-.0189	.0005
25.	-.0185	.0009
30.	-.0181	.0013
35.	-.0177	.0017
40.	-.0172	.0023
45.	-.0166	.0028
50.	-.0159	.0035
55.	-.0153	.0042
60.	-.0145	.0049
65.	-.0138	.0056
70.	-.0130	.0064
75.	-.0122	.0072
80.	-.0113	.0081
85.	-.0105	.0089
90.	-.0096	.0098
95.	-.0088	.0106
100.	-.0079	.0115
105.	-.0071	.0123
110.	-.0063	.0131
115.	-.0055	.0139
120.	-.0047	.0147
125.	-.0040	.0154
130.	-.0033	.0161
135.	-.0027	.0167
140.	-.0022	.0173
145.	-.0016	.0178
150.	-.0012	.0182
155.	-.0008	.0186
160.	-.0005	.0189
165.	-.0002	.0192
170.	-.0001	.0193
175.	0.0000	.0194
180.	0.0000	.0195

TABLE XII

ANGLE	ADNSF	ADSF	BDNSF	BDSF
0.	.1077	0.0000	0.0000	0.0000
5.	.0522	.0025	.0201	.0001
10.	.0294	.0033	.0249	.0002
15.	.0217	.0035	.0244	.0003
20.	.0166	.0036	.0225	.0005
25.	.0129	.0035	.0205	.0008
30.	.0101	.0033	.0187	.0011
35.	.0083	.0030	.0167	.0015
40.	.0066	.0028	.0147	.0018
45.	.0052	.0028	.0130	.0022
50.	.0042	.0027	.0112	.0026
55.	.0033	.0026	.0096	.0030
60.	.0027	.0025	.0083	.0033
65.	.0022	.0025	.0070	.0039
70.	.0018	.0023	.0060	.0044
75.	.0016	.0022	.0049	.0047
80.	.0013	.0022	.0041	.0051
85.	.0011	.0022	.0032	.0054
90.	.0008	.0021	.0027	.0057
95.	.0007	.0021	.0022	.0060
100.	.0006	.0021	.0018	.0062
105.	.0005	.0021	.0015	.0065
110.	.0003	.0021	.0012	.0067
115.	.0002	.0020	.0008	.0070
120.	.0002	.0020	.0006	.0071
125.	.0002	.0020	.0005	.0073
130.	.0001	.0020	.0003	.0075
135.	.0001	.0020	.0001	.0076

TABLE XIII

ANGLE	ARNSF	ARSF	BRNSF	BRSF
0.	-1.6989	0.0000	.0474	0.0000
5.	-1.4638	.0079	.0476	-.0023
10.	-1.2641	.0166	.0432	-.0028
15.	-1.0937	.0263	.0355	-.0045
20.	-.8611	.0363	.0248	-.0075
25.	-.6350	.0457	.0221	-.0098
30.	-.3946	.0508	.0181	-.0106
35.	-.2429	.0529	.0161	-.0110
40.	-.1613	.0536	.0146	-.0111
45.	-.1149	.0529	.0133	-.0106
50.	-.0803	.0522	.0128	-.0100
55.	-.0496	.0509	.0122	-.0093
60.	-.0226	.0497	.0119	-.0090
65.	-.0127	.0483	.0113	-.0080
70.	-.0035	.0470	.0106	-.0073
75.	.0045	.0458	.0108	-.0072
80.	.0094	.0451	.0099	-.0062
85.	.0110	.0443	.0093	-.0059
90.	.0117	.0440	.0083	-.0055
95.	.0117	.0439	.0080	-.0054
100.	.0112	.0438	.0073	-.0053
105.	.0103	.0437	.0066	-.0053
110.	.0094	.0437	.0059	-.0051
115.	.0085	.0434	.0052	-.0050
120.	.0076	.0429	.0046	-.0048
125.	.0066	.0432	.0036	-.0048
130.	.0057	.0437	.0028	-.0048
135.	.0047	.0443	.0020	-.0049
140.	.0037	.0435	.0018	-.0047
145.	.0029	.0435	.0016	-.0046
150.	.0023	.0445	.0014	-.0045
155.	.0021	.0435	.0012	-.0044
160.	.0019	.0432	.0010	-.0044
165.	.0019	.0433	.0008	-.0041
170.	.0017	.0431	.0006	-.0045
175.	.0016	.0432	.0004	-.0045
180.	0.0000	.0427	0.0000	-.0048

TABLE XIV

ANGLE	CRNSF	CRSF	DRNSF	DRSF
0.	-1.6938	0.0000	.0473	0.0000
5.	-1.4261	.0077	.0464	-.0022
10.	-1.1658	.0152	.0399	-.0027
15.	-.9383	.0225	.0305	-.0039
20.	-.6841	.0288	.0216	-.0059
25.	-.4685	.0337	.0163	-.0072
30.	-.2721	.0351	.0125	-.0073
35.	-.1575	.0345	.0106	-.0072
40.	-.0989	.0332	.0091	-.0069
45.	-.0670	.0314	.0079	-.0063
50.	-.0447	.0297	.0074	-.0057
55.	-.0262	.0280	.0068	-.0051
60.	-.0107	.0265	.0064	-.0047
65.	-.0053	.0250	.0059	-.0042
70.	-.0004	.0237	.0055	-.0038
75.	.0035	.0226	.0055	-.0036
80.	.0058	.0217	.0049	-.0031
85.	.0065	.0209	.0046	-.0028
90.	.0066	.0203	.0040	-.0026
95.	.0064	.0199	.0038	-.0025
100.	.0061	.0197	.0034	-.0024
105.	.0056	.0193	.0031	-.0024
110.	.0050	.0190	.0027	-.0023
115.	.0044	.0186	.0023	-.0022
120.	.0039	.0182	.0021	-.0022
125.	.0034	.0183	.0016	-.0022
130.	.0029	.0181	.0012	-.0022
135.	.0023	.0182	.0009	-.0022
140.	.0018	.0177	.0008	-.0021
145.	.0014	.0176	.0007	-.0021
150.	.0011	.0180	.0006	-.0020
155.	.0010	.0174	.0005	-.0020
160.	.0009	.0172	.0004	-.0020
165.	.0008	.0171	.0003	-.0018
170.	.0007	.0170	.0002	-.0020
175.	.0006	.0170	.0001	-.0020
180.	0.0000	.0168	0.0000	-.0021

TABLE XV

ANGLE	ARLNSF	ARLSF	BRLNSF	BRLSF
0.	-6.7956	0.0000	.1896	0.0000
5.	-3.7943	.0204	.1233	-.0059
10.	-1.0490	.0137	.0358	-.0023
15.	-.2050	.0049	.0066	-.0008
20.	-.0677	.0028	.0019	-.0005
25.	-.0618	.0044	.0021	-.0009
30.	-.0512	.0066	.0023	-.0013
35.	-.0377	.0082	.0025	-.0017
40.	-.0278	.0092	.0025	-.0019
45.	-.0212	.0097	.0024	-.0019
50.	-.0154	.0100	.0024	-.0019
55.	-.0098	.0100	.0024	-.0018
60.	-.0045	.0100	.0024	-.0018
65.	-.0025	.0098	.0023	-.0016
70.	-.0007	.0097	.0021	-.0015
75.	.0009	.0095	.0022	-.0014
80.	.0019	.0094	.0020	-.0012
85.	.0023	.0093	.0019	-.0012
90.	.0024	.0092	.0017	-.0011
95.	.0024	.0092	.0016	-.0011
100.	.0023	.0092	.0015	-.0011
105.	.0021	.0092	.0014	-.0011
110.	.0019	.0092	.0012	-.0010
115.	.0018	.0092	.0011	-.0010
120.	.0016	.0091	.0009	-.0010
125.	.0014	.0092	.0007	-.0010
130.	.0012	.0093	.0005	-.0010
135.	.0010	.0094	.0004	-.0010
140.	.0007	.0092	.0003	-.0010
145.	.0006	.0092	.0003	-.0009
150.	.0004	.0095	.0002	-.0009
155.	.0004	.0092	.0002	-.0009
160.	.0004	.0092	.0002	-.0009
165.	.0004	.0092	.0001	-.0008
170.	.0003	.0092	.0001	-.0009
175.	.0003	.0092	0.0000	-.0009
180.	0.0000	.0091	0.0000	-.0010

APPENDIX III

This appendix lists the various theoretical elastic scattering cross sections. All cross sections are given in millibarns per steradian.

```
      DIMENSION ARNSF(37),ARSF(37),BRNSF(37),BRSF(37),ADNSF(37),
     1 BDSF(37),BDNSF(37),CRNSF(37),CRSF(37),DRNSF(37),DRSF(37)
      DIMENSION RATIO(37),ANGS(38),ANGR(37),CRSCA(37),CRSCB(37),
     1 CRSCC(37),ADSF(37),ATNSF(37),ATSF(37)
      READ 70,Z,RAT
70    FORMAT(F4.0,F9.5)
      READ 10,(ARNSF(I),I=1,37)
      READ 10,(ARSF(I),I=1,37)
      READ 10,(BRNSF(I),I=1,37)
      READ 10,(BRSF(I),I=1,37)
      READ 10,(ADNSF(I),I=1,37)
      READ 10,(ADSF(I),I=1,37)
      READ 10,(BDNSF(I),I=1,37)
      READ 10,(BDSF(I),I=1,37)
      READ 10,(CRNSF(I),I=1,37)
      READ 10,(CRSF(I),I=1,37)
      READ 10,(DRNSF(I),I=1,37)
      READ 10,(DRSF(I),I=1,37)
      READ 10,(RATIO(I),I=1,37)
10    FORMAT(11F7.4)
      ANGS(1)=0.
      DO 20 I=1,37
      ANGR(I)=.017543*ANGS(I)
      ATNSF(I)=(-.0002723)*(Z**2)*(COSF(ANGR(I))+1.)/RAT
      ATSF(I)=(-.0002723)*(Z**2)*(COSF(ANGR(I))-1.)/RAT
20    ANGS(I+1)=ANGS(I)+5.
      DO 30 I=1,37
      CRSCA(I)=((ATNSF(I)+ARNSF(I))**2+(ATSF(I)+ARSF(I))**2+BRSF(I)**2
     1 +BRNSF(I)**2)*79.41
      CRSCB(I)=((ATNSF(I)+ADNSF(I)+ARNSF(I))**2+(ATSF(I)+ADSF(I)+ARSF(I)
     1)**2+(BDNSF(I)+BRNSF(I))**2+(BDSF(I)+BRSF(I))**2)*79.41
      CRSCC(I)=((ATNSF(I)+ADNSF(I)+ARNSF(I)+RATIO(I)*ARNSF(I))**2+(ATSF(
     1I)+ADSF(I)+ARSF(I)+RATIO(I)*ARSF(I))**2+(BRNSF(I)+BDNSF(I)+RATIO(I
     1)*BRNSF(I))**2+(BRSF(I)+BDSF(I)+RATIO(I)*BRSF(I))**2)*79.41
30    PUNCH 12,ANGS(I),CRSCA(I),CRSCB(I),CRSCC(I)
12    FORMAT(F6.0,3E14.7)
      DO 40 I=1,37
```

```
      CRSCA(I)=((ATNSF(I)+ADNSF(I)+ARNSF(I))**2+(ATSF(I)+ADSF(I)+ARSF(I)
     1+RATIO(I)*ARSF(I))**2+(BRNSF(I)+BDNSF(I))**2+(BRSF(I)+BDSF(I)+
     1 RATIO(I)*BRSF(I))**2)*79.41
      CRSCB(I)=((ATNSF(I)+ARNSF(I)+RATIO(I)*ARNSF(I))**2+(ATSF(I)+ARSF(I
     1)+ARSF(I)*RATIO(I))**2+(BRNSF(I)+RATIO(I)*BRNSF(I))**2+(BRSF(I)+RA
     1TIO(I)*BRSF(I))**2)*79.41
      CRSCC(I)=((ATNSF(I)+ADNSF(I))**2+((1.+RATIO(I))*ARNSF(I))**2+(ATSF
     1(I)+ADSF(I))**2+((1.+RATIO(I))*ARSF(I))**2+(ADNSF(I))**2+((1.+RATI
     1 O(I))*BRNSF(I))**2+BDSF(I)**2+((1.+RATIO(I))*BRSF(I))**2)*79.41
   40 PUNCH 12,ANGS(I),CRSCA(I),CRSCB(I),CRSCC(I)
      DO 50 I=1,37
      CRSCA(I)=((ATNSF(I)+CRNSF(I))**2+(ATSF(I)+CRSF(I))**2+DRSF(I)**2
     1 +DRNSF(I)**2)*79.4
      CRSCB(I)=((ATNSF(I)+ADNSF(I)+CRNSF(I))**2+(ATSF(I)+ADSF(I)+CRSF(I)
     1)**2+(BDNSF(I)+DRNSF(I))**2+(BDSF(I)+DRSF(I))**2)*79.41
      CRSCC(I)=((ATNSF(I)+ADNSF(I)+CRNSF(I)+RATIO(I)*CRNSF(I))**2+(ATSF(
     1I)+ADSF(I)+CRSF(I)+RATIO(I)*CRSF(I))**2+(DRNSF(I)+BDNSF(I)+RATIO(I
     1)*DRNSF(I))**2+(DRSF(I)+BDSF(I)+RATIO(I)*DRSF(I))**2)*79.41
   50 PUNCH 12,ANGS(I),CRSCA(I),CRSCB(I),CRSCC(I)
      DO 60 I=1,37
      CRSCA(I)=((ATNSF(I)+ADNSF(I)+CRNSF(I))**2+(ATSF(I)+ADSF(I)+CRSF(I)
     1+RATIO(I)*CRSF(I))**2+(DRNSF(I)+BDNSF(I))**2+(DRSF(I)+BDSF(I)+
     1 RATIO(I)*DRSF(I))**2)*79.41
      CRSCB(I)=((ATNSF(I)+CRNSF(I)+RATIO(I)*CRNSF(I))**2+(ATSF(I)+CRSF(I
     1)+CRSF(I)*RATIO(I))**2+(DRNSF(I)+RATIO(I)*DRNSF(I))**2+(DRSF(I)+RA
     1TIO(I)*DRSF(I))**2)*79.41
      CRSCC(I)=((ATNSF(I)+ADNSF(I))**2+((1.+RATIO(I))*CRNSF(I))**2+(ATSF
     1(I)+ADSF(I))**2+((1.+RATIO(I))*CRSF(I))**2+(ADNSF(I))**2+((1.+RATI
     1 O(I))*DRNSF(I))**2+BDSF(I)**2+((1.+RATIO(I))*DRSF(I))**2)*79.41
   60 PUNCH 12,ANGS(I),CRSCA(I),CRSCB(I),CRSCC(I)
      CALL EXIT
      END
```

TABLE XXIV

ANGLE	CRSCA	CRSCB	CRSCC
0.	2.3420843E+02	2.1145160E+02	5.6433269E+03
5.	1.6949222E+02	1.6014720E+02	1.7344837E+03
10.	1.0288112E+02	9.8865029E+01	2.2345243E+02
15.	7.9475346E+01	7.6891850E+01	8.8594433E+01
20.	4.4443223E+01	4.2996658E+01	4.8335732E+01
25.	2.2101318E+01	2.1332850E+01	2.5828513E+01
30.	8.1371800E+00	7.8012021E+00	9.9616049E+00
35.	3.1077145E+00	2.9619857E+00	3.8856390E+00
40.	1.4539794E+00	1.3911224E+00	1.8425559E+00
45.	8.1795277E-01	7.9334770E-01	1.0511785E+00
50.	4.8157501E-01	4.7590021E-01	6.2685462E-01
55.	2.7944262E-01	2.8534749E-01	3.7160931E-01
60.	1.6754872E-01	1.7948758E-01	2.3146738E-01
65.	1.3548310E-01	1.4827932E-01	1.9072595E-01
70.	1.1385684E-01	1.2657652E-01	1.6275183E-01
75.	1.0144151E-01	1.1349062E-01	1.4628260E-01
80.	9.6507092E-02	1.0850551E-01	1.3988199E-01
85.	9.4770141E-02	1.0620730E-01	1.3651588E-01
90.	9.5693055E-02	1.0632731E-01	1.3618932E-01
95.	9.7933025E-02	1.0842034E-01	1.3827069E-01
100.	1.0014383E-01	1.1055924E-01	1.4029386E-01
105.	1.0241519E-01	1.1278712E-01	1.4232227E-01
110.	1.0521147E-01	1.1569494E-01	1.4525440E-01
115.	1.0732544E-01	1.1724871E-01	1.4651596E-01
120.	1.0883701E-01	1.1884209E-01	1.4772961E-01
125.	1.1370935E-01	1.2390778E-01	1.5357641E-01
130.	1.1727654E-01	1.2767600E-01	1.5770625E-01
135.	1.2192364E-01	1.3251261E-01	1.6330068E-01
140.	1.2199394E-01	1.2199394E-01	1.5142340E-01
145.	1.2427217E-01	1.2427217E-01	1.5381541E-01
150.	1.2999604E-01	1.2999604E-01	1.6085651E-01
155.	1.2840072E-01	1.2840072E-01	1.5827361E-01
160.	1.2895984E-01	1.2895984E-01	1.5862050E-01
165.	1.3033641E-01	1.3033641E-01	1.6012583E-01
170.	1.3078096E-01	1.3078096E-01	1.6050137E-01
175.	1.3006883E-01	1.3006883E-01	1.5943719E-01
180.	1.3019547E-01	1.3019547E-01	1.5957291E-01

TABLE XVI

ANGLE	CRSCD	CRSCE	CRSCF
0.	2.1145160E+02	5.7584697E+03	5.7353570E+03
5.	1.6020316E+02	1.7649869E+03	1.7518874E+03
10.	9.8893854E+01	2.2948658E+02	2.2478826E+02
15.	7.6899635E+01	9.1368280E+01	8.8435565E+01
20.	4.3007420E+01	4.9870347E+01	4.7736422E+01
25.	2.1358763E+01	2.6675573E+01	2.5148773E+01
30.	7.8398843E+00	1.0343092E+01	9.4253579E+00
35.	3.0065188E+00	4.0541944E+00	3.5083376E+00
40.	1.4376407E+00	1.9161307E+00	1.5649726E+00
45.	8.3843261E-01	1.0803526E+00	8.3605142E-01
50.	5.1880304E-01	6.3376256E-01	4.6443997E-01
55.	3.2540091E-01	3.6487566E-01	2.5509943E-01
60.	2.1726209E-01	2.1759678E-01	1.5427824E-01
65.	1.8355668E-01	1.7588830E-01	1.2790686E-01
70.	1.5970209E-01	1.4805869E-01	1.1222426E-01
75.	1.4475045E-01	1.3240362E-01	1.0516552E-01
80.	1.3874099E-01	1.2615456E-01	1.0202422E-01
85.	1.3546124E-01	1.2353516E-01	9.8331060E-02
90.	1.3530953E-01	1.2425966E-01	9.6113964E-02
95.	1.3740213E-01	1.2659049E-01	9.4691406E-02
100.	1.3952926E-01	1.2878678E-01	9.2996479E-02
105.	1.4171368E-01	1.3095395E-01	9.1132702E-02
110.	1.4475960E-01	1.3384178E-01	9.0209966E-02
115.	1.4615573E-01	1.3580989E-01	8.8684579E-02
120.	1.4744469E-01	1.3697674E-01	8.6941387E-02
125.	1.5337300E-01	1.4264504E-01	8.8601731E-02
130.	1.5758101E-01	1.4661226E-01	8.9518503E-02
135.	1.6323406E-01	1.5202747E-01	9.1442084E-02
140.	1.5137941E-01	1.5142340E-01	8.2550030E-02
145.	1.5378407E-01	1.5381541E-01	8.2866614E-02
150.	1.6082870E-01	1.6085651E-01	8.6340213E-02
155.	1.5824326E-01	1.5827361E-01	8.4021592E-02
160.	1.5859398E-01	1.5862050E-01	8.3693002E-02
165.	1.6009550E-01	1.6012583E-01	8.4185812E-02
170.	1.6047457E-01	1.6050137E-01	8.4181723E-02
175.	1.5941516E-01	1.5943719E-01	8.3386916E-02
180.	1.5957291E-01	1.5957291E-01	8.3426668E-02

TABLE XVII

ANGLE	CRSCG	CRSCH	CRSCI
0.	2.3325222E+02	2.1057098E+02	5.6205794E+03
5.	1.6612150E+02	1.5689166E+02	1.6996128E+03
10.	1.1167490E+02	1.0749160E+02	2.4293131E+02
15.	7.2912069E+01	7.0448627E+01	8.1169733E+01
20.	3.9345752E+01	3.7991531E+01	4.2706713E+01
25.	1.8965028E+01	1.8257465E+01	2.2099614E+01
30.	6.8136794E+00	6.5087020E+00	8.3046588E+00
35.	2.5568791E+00	2.4263665E+00	3.1771015E+00
40.	1.1827326E+00	1.1269968E+00	1.4877228E+00
45.	6.5715783E-01	6.3584206E-01	8.3814285E-01
50.	3.8708459E-01	3.8246070E-01	5.0032272E-01
55.	2.2434594E-01	2.2977083E-01	2.9656289E-01
60.	1.3467001E-01	1.4527745E-01	1.8533480E-01
65.	1.0799187E-01	1.1929449E-01	1.5158051E-01
70.	9.0024434E-02	1.0125459E-01	1.2844632E-01
75.	8.0311726E-02	9.1030517E-02	1.1568144E-01
80.	7.6248942E-02	8.6938758E-02	1.1045360E-01
85.	7.4562400E-02	8.4859090E-02	1.0743418E-01
90.	7.4856301E-02	8.4507709E-02	1.0652224E-01
95.	7.6757852E-02	8.6336854E-02	1.0831390E-01
100.	7.9110945E-02	8.8721561E-02	1.1078049E-01
105.	8.1186714E-02	9.0763660E-02	1.1269410E-01
110.	8.3640714E-02	9.3381927E-02	1.1534622E-01
115.	8.5562226E-02	9.4872095E-02	1.1660330E-01
120.	8.6968558E-02	9.6304842E-02	1.1772766E-01
125.	9.0781886E-02	1.0030246E-01	1.2223276E-01
130.	9.3455372E-02	1.0318367E-01	1.2525186E-01
135.	9.7628143E-02	1.0756553E-01	1.3030079E-01
140.	9.7693283E-02	9.7705587E-02	1.1929127E-01
145.	9.9730894E-02	9.9743454E-02	1.2142395E-01
150.	1.0486227E-01	1.0487548E-01	1.2769068E-01
155.	1.0342438E-01	1.0343740E-01	1.2538530E-01
160.	1.0393161E-01	1.0394470E-01	1.2570350E-01
165.	1.0516934E-01	1.0518259E-01	1.2704693E-01
170.	1.0556341E-01	1.0557670E-01	1.2737541E-01
175.	1.0608074E-01	1.0609410E-01	1.2794047E-01
180.	1.0505499E-01	1.0506822E-01	1.2657349E-01

TABLE XVIII

ANGLE	CRSCJ	CRSCK	CRSCL
0.	2.1057098E+02	5.7354911E+03	5.7124265E+03
5.	1.5694603E+02	1.7298092E+03	1.7168428E+03
10.	1.0751905E+02	2.4923761E+02	2.4433782E+02
15.	7.0455740E+01	8.3824560E+01	8.1017599E+01
20.	3.8001109E+01	4.4148635E+01	4.2143192E+01
25.	1.8279688E+01	2.2882195E+01	2.1470755E+01
30.	6.5409351E+00	8.6519529E+00	7.8154780E+00
35.	2.4626634E+00	3.3284570E+00	2.8369089E+00
40.	1.1640982E+00	1.5531597E+00	1.2400442E+00
45.	6.7124222E-01	8.6354920E-01	6.4827460E-01
50.	4.1579744E-01	5.0604823E-01	3.5764810E-01
55.	2.6054635E-01	2.9043052E-01	1.9504834E-01
60.	1.7421719E-01	1.7306242E-01	1.1856375E-01
65.	1.4601312E-01	1.3853161E-01	9.7752495E-02
70.	1.2609073E-01	1.1553603E-01	8.5510125E-02
75.	1.1456707E-01	1.0339570E-01	8.0554830E-02
80.	1.0976031E-01	9.8293801E-02	7.8257906E-02
85.	1.0681242E-01	9.5821331E-02	7.5205020E-02
90.	1.0604069E-01	9.5766157E-02	7.2905433E-02
95.	1.0785373E-01	9.7726210E-02	7.1683140E-02
100.	1.1038545E-01	1.0024320E-01	7.0979559E-02
105.	1.1237517E-01	1.0228432E-01	6.9804132E-02
110.	1.1509783E-01	1.0482981E-01	6.9308873E-02
115.	1.1643715E-01	1.0664036E-01	6.8251621E-02
120.	1.1758531E-01	1.0778416E-01	6.7168120E-02
125.	1.2213984E-01	1.1212211E-01	6.8391636E-02
130.	1.2520533E-01	1.1497107E-01	6.8991968E-02
135.	1.3027963E-01	1.1981811E-01	7.0890782E-02
140.	1.1928263E-01	1.1929127E-01	6.2518957E-02
145.	1.2141607E-01	1.2142395E-01	6.3003328E-02
150.	1.2767990E-01	1.2769068E-01	6.6067021E-02
155.	1.2537145E-01	1.2538530E-01	6.4311513E-02
160.	1.2568892E-01	1.2570350E-01	6.4189026E-02
165.	1.2702925E-01	1.2704693E-01	6.4702103E-02
170.	1.2736020E-01	1.2737541E-01	6.4779102E-02
175.	1.2792860E-01	1.2794047E-01	6.5013663E-02
180.	1.2657349E-01	1.2657349E-01	6.4241405E-02

TABLE XIX

ANGLE	CRSCA	CRSCB	CRSCC
0.	2.3467334E+02	2.0620105E+02	5.6160637E+03
5.	1.7489724E+02	1.6300429E+02	2.1712533E+03
10.	1.3098269E+02	1.2528807E+02	4.2217978E+02
15.	9.8508025E+01	9.4910427E+01	1.3388163E+02
20.	6.1659964E+01	5.9512110E+01	6.9204519E+01
25.	3.4141972E+01	3.2947135E+01	3.9597740E+01
30.	1.3782338E+01	1.3236227E+01	1.6804051E+01
35.	5.6620834E+00	5.4131566E+00	7.1360589E+00
40.	2.8054673E+00	2.6956199E+00	3.6274457E+00
45.	1.6439679E+00	1.6004784E+00	2.1738608E+00
50.	1.0039117E+00	9.9468600E-01	1.3534458E+00
55.	5.9445030E-01	6.0678403E-01	8.2179614E-01
60.	3.6448665E-01	3.8860662E-01	5.2429312E-01
65.	3.0257078E-01	3.2832264E-01	4.4367241E-01
70.	2.6199427E-01	2.8687428E-01	3.8914715E-01
75.	2.4199570E-01	2.6586449E-01	3.6271938E-01
80.	2.3618477E-01	2.5971849E-01	3.5525144E-01
85.	2.3510258E-01	2.5707666E-01	3.5137225E-01
90.	2.3837273E-01	2.5872569E-01	3.5291651E-01
95.	2.4472781E-01	2.6453698E-01	3.5978873E-01
100.	2.5048578E-01	2.6980669E-01	3.6552114E-01
105.	2.5617160E-01	2.7512893E-01	3.7112597E-01
110.	2.6256779E-01	2.8142137E-01	3.7796031E-01
115.	2.6623831E-01	2.8392162E-01	3.7980732E-01
120.	2.6787711E-01	2.8565028E-01	3.8034849E-01
125.	2.7649335E-01	2.9449548E-01	3.9083730E-01
130.	2.8703415E-01	3.0528014E-01	4.0414541E-01
135.	2.9842819E-01	3.1687200E-01	4.1871976E-01
140.	2.9587636E-01	2.9587636E-01	3.9351631E-01
145.	3.0065520E-01	3.0065520E-01	3.9895113E-01
150.	3.1480041E-01	3.1480041E-01	4.1762772E-01
155.	3.0861798E-01	3.0861798E-01	4.0804049E-01
160.	3.0876796E-01	3.0876796E-01	4.0746752E-01
165.	3.1201509E-01	3.1201509E-01	4.1142031E-01
170.	3.1198765E-01	3.1198765E-01	4.1096965E-01
175.	3.1394537E-01	3.1394537E-01	4.1344751E-01
180.	3.0923277E-01	3.0923277E-01	4.0682994E-01

TABLE XX

ANGLE	CRSCD	CRSCE	CRSCF
0.	2.0620105E+02	5.7607740E+03	5.7359489E+03
5.	1.6307644E+02	2.2142007E+03	2.1982030E+03
10.	1.2534840E+02	4.3262392E+02	4.2555503E+02
15.	9.4936584E+01	1.3815747E+02	1.3420868E+02
20.	5.9531814E+01	7.1522479E+01	6.8722205E+01
25.	3.2985579E+01	4.0909930E+01	3.8834391E+01
30.	1.3300048E+01	1.7422241E+01	1.6110079E+01
35.	5.4966448E+00	7.4245982E+00	6.6060310E+00
40.	2.7919738E+00	3.7570605E+00	3.2076051E+00
45.	1.7018292E+00	2.2261394E+00	1.8307058E+00
50.	1.0984933E+00	1.3650856E+00	1.0817174E+00
55.	7.0926321E-01	8.0764321E-01	6.1909891E-01
60.	4.8949442E-01	4.9593295E-01	3.8447256E-01
65.	4.2595974E-01	4.1335046E-01	3.2709812E-01
70.	3.8125837E-01	3.5989393E-01	2.9390140E-01
75.	3.5755513E-01	3.3465186E-01	2.8306857E-01
80.	3.5021279E-01	3.2771706E-01	2.8102979E-01
85.	3.4619188E-01	3.2581245E-01	2.7579421E-01
90.	3.4802944E-01	3.2945600E-01	2.7307530E-01
95.	3.5493227E-01	3.3710626E-01	2.7253088E-01
100.	3.6121024E-01	3.4354348E-01	2.7000742E-01
105.	3.6752044E-01	3.4972966E-01	2.6709493E-01
110.	3.7503779E-01	3.5682972E-01	2.6534386E-01
115.	3.7749044E-01	3.6017619E-01	2.6091239E-01
120.	3.7848191E-01	3.6068181E-01	2.5481730E-01
125.	3.8952539E-01	3.7099218E-01	2.5694768E-01
130.	4.0324313E-01	3.8411209E-01	2.6197779E-01
135.	4.1816120E-01	3.9851422E-01	2.6828668E-01
140.	3.9315802E-01	3.9351631E-01	2.4995576E-01
145.	3.9870606E-01	3.9895113E-01	2.5045829E-01
150.	4.1745256E-01	4.1762772E-01	2.6143031E-01
155.	4.0788204E-01	4.0804049E-01	2.5193637E-01
160.	4.0732942E-01	4.0746752E-01	2.4966004E-01
165.	4.1127982E-01	4.1142031E-01	2.5109596E-01
170.	4.1085475E-01	4.1096965E-01	2.4988406E-01
175.	4.1334674E-01	4.1344751E-01	2.5113463E-01
180.	4.0682994E-01	4.0682994E-01	2.4619291E-01

TABLE XXI

ANGLE	CRSCG	CRSCH	CRSCI
0.	2.3325339E+02	2.0489771E+02	5.5820517E+03
5.	1.6609878E+02	1.5453539E+02	2.0601897E+03
10.	1.1167304E+02	1.0643769E+02	3.5884183E+02
15.	7.2908363E+01	6.9834035E+01	9.8510971E+01
20.	3.9351372E+01	3.7659522E+01	4.3783918E+01
25.	1.8959013E+01	1.8082462E+01	2.1715393E+01
30.	6.8132585E+00	6.4402213E+00	8.1534281E+00
35.	2.5557695E+00	2.3972902E+00	3.1379777E+00
40.	1.1809497E+00	1.1159477E+00	1.4813454E+00
45.	6.5680644E-01	6.3375084E-01	8.4264912E-01
50.	3.8709374E-01	3.8418540E-01	5.0749401E-01
55.	2.2493404E-01	2.3387196E-01	3.0461028E-01
60.	1.3421692E-01	1.4924864E-01	1.9188167E-01
65.	1.0799843E-01	1.2344853E-01	1.5816571E-01
70.	9.0207594E-02	1.0505995E-01	1.3452667E-01
75.	8.0442283E-02	9.4523589E-02	1.2138114E-01
80.	7.5817550E-02	8.9696628E-02	1.1509630E-01
85.	7.4500802E-02	8.7792035E-02	1.1226505E-01
90.	7.4681982E-02	8.7273273E-02	1.1099503E-01
95.	7.6423696E-02	8.8944703E-02	1.1251301E-01
100.	7.9147770E-02	9.1695449E-02	1.1539152E-01
105.	8.1069083E-02	9.3685416E-02	1.1710437E-01
110.	8.3403387E-02	9.6189444E-02	1.1943357E-01
115.	8.5163661E-02	9.7594405E-02	1.2041166E-01
120.	8.6898488E-02	9.9412950E-02	1.2192536E-01
125.	9.1048337E-02	1.0390663E-01	1.2699085E-01
130.	9.3495596E-02	1.0659806E-01	1.2964728E-01
135.	9.7419853E-02	1.1078891E-01	1.3438999E-01
140.	9.7758018E-02	9.7770330E-02	1.2007343E-01
145.	1.0004561E-01	1.0005821E-01	1.2248735E-01
150.	1.0483809E-01	1.0485129E-01	1.2832806E-01
155.	1.0359296E-01	1.0360601E-01	1.2614609E-01
160.	1.0426146E-01	1.0427459E-01	1.2661495E-01
165.	1.0504262E-01	1.0505585E-01	1.2732732E-01
170.	1.0552472E-01	1.0553801E-01	1.2774195E-01
175.	1.0609262E-01	1.0610599E-01	1.2836318E-01
180.	1.0507896E-01	1.0509219E-01	1.2697883E-01

TABLE XXII

ANGLE	CRSCJ	CRSCK	CRSCL
0.	2.0489771E+02	5.7263258E+03	5.7015797E+03
5.	1.5460395E+02	2.1020285E+03	2.0864499E+03
10.	1.0648897E+02	3.6847128E+02	3.6195580E+02
15.	6.9853554E+01	1.0217633E+02	9.8789994E+01
20.	3.7672222E+01	4.5615331E+01	4.3389686E+01
25.	1.8103943E+01	2.2680918E+01	2.1146941E+01
30.	6.4716662E+00	8.5770121E+00	7.6686646E+00
35.	2.4341334E+00	3.3223857E+00	2.7877885E+00
40.	1.1545660E+00	1.5585354E+00	1.2179295E+00
45.	6.7142504E-01	8.7081974E-01	6.3695455E-01
50.	4.2003263E-01	5.1165843E-01	3.5116424E-01
55.	2.6735472E-01	2.9455914E-01	1.9251259E-01
60.	1.8061550E-01	1.7446407E-01	1.1796224E-01
65.	1.5257014E-01	1.4026863E-01	9.8945026E-02
70.	1.3219546E-01	1.1738652E-01	8.8070939E-02
75.	1.2016838E-01	1.0515012E-01	8.3704333E-02
80.	1.1425654E-01	9.9247880E-02	8.1241956E-02
85.	1.1148236E-01	9.7223695E-02	7.8492696E-02
90.	1.1039162E-01	9.6943743E-02	7.5907513E-02
95.	1.1192183E-01	9.8671062E-02	7.4470766E-02
100.	1.1488546E-01	1.0163375E-01	7.3794202E-02
105.	1.1667452E-01	1.0340701E-01	7.2435952E-02
110.	1.1913663E-01	1.0567199E-01	7.1545118E-02
115.	1.2022256E-01	1.0716333E-01	7.0274814E-02
120.	1.2175391E-01	1.0865024E-01	6.9459119E-02
125.	1.2688066E-01	1.1339911E-01	7.0942011E-02
130.	1.2959006E-01	1.1586786E-01	7.1406088E-02
135.	1.3436675E-01	1.2035601E-01	7.3049262E-02
140.	1.2006244E-01	1.2007343E-01	6.1784279E-02
145.	1.2247578E-01	1.2248735E-01	6.2481450E-02
150.	1.2831549E-01	1.2832806E-01	6.5187726E-02
155.	1.2612827E-01	1.2614609E-01	6.3730914E-02
160.	1.2659508E-01	1.2661495E-01	6.3799195E-02
165.	1.2730796E-01	1.2732732E-01	6.4015027E-02
170.	1.2772498E-01	1.2774195E-01	6.4205427E-02
175.	1.2834980E-01	1.2836318E-01	6.4489934E-02
180.	1.2697883E-01	1.2697883E-01	6.3777391E-02

BIBLIOGRAPHY

1. Eisberg, R. M., Fundamentals of Modern Physics, New York: John Wiley and Sons, Inc., 1961, pp. 503.

2. Berstein, A. M., and Mann, A. K., "Scattering of Gamma Rays by a Static Electric Field", Physical Review, CX (1958), pp. 805-814.

3. Levinger, J. S., "Elastic Scattering of Photons by Nuclei", Physical Review, LXXXIV (1951), 523-524.

4. Chiang, C. K., "Elastic Scattering of 1.33 MeV Gamma Rays from Lead", unpublished Master's Thesis, Western Michigan University, Kalamazoo, Michigan, August, 1970.

5. Evans, R. D., The Atomic Nucleus, New York: McGraw Hill Book Co. Inc., pp. 672-745.

6. Schwandt, D. R., "Elastic Scattering of 1.33 MeV Gamma Rays from Uranium", unpublished Master's Thesis, Western Michigan University, Kalamazoo, Michigan, April, 1969.

7. Learn, L., "The Elastic Scattering of 1.17 MeV and 1.33 MeV Gamma Rays from Lead at 29°", unpublished Master's Thesis, Western Michigan University, Kalamazoo, Michigan, August, 1967.

8. Colgate, S. A., "Gamma-Ray Absorption Measurements", Physical Review, LXXXVII (1952), pp. 592-601.

9. Grodstein, G. W., X-ray Attenuation Coefficients From 10 kev to 100 Mev, National Bureau of Standards Circular 583, U. S. Government Printing Office, Washington, D. C., 1957, pp. 46.

10. Eberhard, P. and Goldzahl, L., "Diffusion des Rayons du ^{60}Co par le Champ Electrique des Noyaux", Academie des Sciences, CCXL (1955), pp. 2305-2306.

11. Ehlotsky, F. and Sheppey, C. G., "Numerical Calculations of the Delbruck Scattering Amplitudes", Nuovo Cimento, XXXIII (1965), pp. 85-87.

12. Brown, G. E., and Mayers, D. F., "Scattering of 1.28 and 2.56 m_0c^2 Gamma Rays in Mercury", Proceedings of the Royal Society, A, CCXLII (1957), pp. 89-95.

13. Kittel, C., Introduction to Solid State Physics, New York: John Wiley and Sons, Inc., 1968, pp. 66-67.

14. Anand, S. and Sood, B. S., "Measurement of Z Dependence of Elastic Scattering Cross Section of Gamma Rays", Nuclear Physics, LXXIII (1965), pp. 368-378.

15. Woodward, J. B., "The Coherent Scattering of Gamma Rays by Bound Electrons", unpublished Doctoral Thesis, University of Birmingham, Birmingham, England, May, 1955.

16. Hardie, G., Merrow, W. J., and Schwandt, D. R., "Large-Angle Scattering of 1.33 MeV Photons from Lead and Uranium, to be published in Physical Review.